Journal of Thermal Analysis and Calorimetry (2023) 148:3929–3954
https://doi.org/10.1007/s10973-023-11991-y

A review of different working fluids used in the receiver tube of parabolic trough solar collector

Asish Sarangi[1] · Abhisek Sarangi[1] · Sudhansu Sekhar Sahoo[1] · Ramesh Kumar Mallik[1] · Subhankar Ray[2] · Shinu M. Varghese[3]

Received: 22 September 2022 / Accepted: 22 January 2023 / Published online: 28 February 2023

Abstract

Parabolic trough solar collectors (PTSCs) or parabolic trough collectors have caught the interest of scientists and renewable energy enthusiasts due to their wide range of operating temperatures between 100 and 700 °C and their potential for power production as well as industrial process heating. More PTSCs have been constructed than all other concentrated sun-producing apparatuses put together. One of the most important functional components of the PTSC is the space for heat collection, also known as the absorber tube and transporting fluids. To increase its thermal potential, numerous investigations on the fluids in the absorber tube flow have been conducted. Better fluid thermo-physical properties are required to improve heat transfer and the system's overall efficiency. Examining different heat transfer fluids (HTF) that have been used for PTSC absorber tube/receiver tube is the goal of the current review. The usage of novel HTFs like nanofluids is also investigated, along with conventional fluids like thermic fluid and water. Review of the performance of the PTSC with various fluids using experiments and numerical methods are presented.. There are many difficulties with once-through PTSCs since two-phase flow circumstances make them worse and can occasionally cause tube bending. Summarized comparisons of several studies looking at the stability, manufacturing methods, and effects of hybrid nanofluids on PTSC thermal properties are summarized. For HTF inside the absorber tube, hybrid nanofluids and nanofluids may be used to enhance the thermal and optical characteristics of PTSC. It also demonstrates that metal oxide hybrid nanofluids are discovered to be more successful and efficient in enhancing thermal conductivity causing heat transfer augmentation than oxide nanofluids. This research, in our opinion, will encourage scientists and manufacturers to choose appropriate working fluids for PTSC applications.

Keywords Concentrated solar power · Parabolic trough solar collectors · Heat transfer fluids · Nanofluids · Thermo-physical properties · Heat transfer augmentation

Abbreviations

CFD	Computational fluid dynamics
CNT	Carbon nanotube
CPC	Compound parabolic concentrator
CTC	Circular trough collectors
CSP	Concentrated solar power
DSC	Differential scanning calorimeter
DSG	Direct steam generation
GNP	Graphene nanoparticles
HDH	Humidification and dehumidification
HTF	Heat transfer fluid
LFR	Linear Fresnel reflector
MWCNT	Multi-wall carbon nanotube
Nm	Nano-meter
PTC	Parabolic trough collector
PTSC	Parabolic trough solar collector
SDC	Solar dish concentrator
TES	Thermal energy storage

List of symbols

h	Flow-induced heat transfer coefficient
K	Thermal conductivity
Nu	Nusselt number
Pr	Prandtl number
Re	Reynolds number
T	Temperature

✉ Sudhansu Sekhar Sahoo
sahoo.sudhansu@gmail.com; sudhansu@cet.edu.in

[1] Department of Mechanical Engineering, Odisha University of Technology and Research, Bhubaneswar, India

[2] School of Mechanical Sciences, Indian Institute of Technology, Bhubaneswar, India

[3] Empereal-KGDS Renewable Energy Pvt. Ltd., Coimbatore 641035, India

Introduction

Importance of renewable energy

Renewable energy is the power that comes from an endless sources. Today's current topic is the efficient use of energy resources. The decision of which energy source to employ and why is crucial. It is necessary to consider a large number of issues, including cleanliness, cost, stability, efficiency, and environmental consequences. It is a sad reality that many sectors still rely on fossil fuels to provide their power. These fuels are indeed quite efficient in terms of the quality of the electricity produced, but they are not beneficial over the long term. Industries must switch as quickly as feasible to renewable energy since fossil fuels will eventually run out. In addition, these fossil fuels constitute a major danger to ecological safety and the environmental balance. Coal, natural gas, and oil are examples of the hydrocarbons that make up fossil fuels. The fundamental problem with fossil fuels is not their consumption, but rather the negative side effects that come along with them. Fossil fuels cannot be used indefinitely. It implies that they will ultimately run out. When they are burned, they release a lot of dangerous gases, carbon dioxide gas being the most notable. The main factor for global warming is this gas. The harmful effects of global warming are continually raising the planet's temperature and putting the lives of its species in threat. Additionally, the persistent melting of ice in the Arctic and Antarctica brought on by these high temperatures is raising sea levels above average. Floods may result from this, which would have a negative impact on fisheries and agriculture. The burning of fossil fuels creates nitrogen monoxide, nitrogen dioxide, sulfur dioxide and carbon monoxide gases. These noxious gases immediately produce air pollution, which is responsible for smog and the deterioration of human health and plant development. Acid rain, which is mostly generated by sulfur dioxide, is highly destructive to marble constructions and crops.

The most important characteristic of renewable energy is its abundance. It is limitless. Renewable energy sources are clean energy sources that have far fewer negative effects on the environment than traditional fossil energy technologies. The majority of renewable energy expenditures are spent on the construction and maintenance of facilities, rather than on expensive energy imports. The field of renewable energy is very young in most nations, and it has the potential to draw a lot of investment from businesses. A pool of new employment might be created for the jobless as a result. As a result, renewable energy has the potential to significantly contribute to reducing unemployment rates in many nations, particularly developing ones. Their economy will therefore see a significant change as a result of this. The use of renewable energy helps stabilize the cost of power. It is because their expenses are independent of shifting prices for coal, oil, and natural gas and solely rely on the initial amount of capital spent.

As a result of technical advances in mass communication, people are more aware of the disadvantages of using fossil fuels. Renewable energy is an urgent need. Its clean and sustainable character has forced humans to consider it carefully. In this field, scientists and engineers from all over the globe are continually working and doing research. They are discovering new methods to use these energy sources efficiently. Global warming is a major threat created by the combustion of coal, oil, and natural gas. It is very destructive to the earth and its inhabitants. Moreover, as previously explained, fossil fuels have been the cause of several unpleasant incidents in the past. To stop this calamity, we must use renewable energy sources. It is because they are less polluting and do not emit toxic gases.

Moreover, fossil fuels are finite. They will eventually come to an end. Therefore, before the critical stage arrives, energy sector specialists must retain a positive outlook and do their utmost to replace fossil fuels with renewable energy sources as the primary source of power generation. Renewable energy is reliable and abundant, and as this technology and its infrastructure are improved, it has the potential to be extremely inexpensive. Solar, wind, biomass, geothermal, hydroelectric, and tidal energy are the primary renewable energy sources. Non-renewable sources of energy, such as coal, natural gas, and oil, need costly explorations and possibly hazardous mining and drilling, and as resources dwindle and energy demand rises, they will become more expensive.

The world's energy consumption is increasing at a startling rate as a result of industrial development, rising mobility, new transportation options, changing lifestyles, and labor automation. Many wealthy countries have lately been pushed to boost their use of cheap solar energy for home and commercial use as well as for power generation due to the environmental implications of using fossil fuels. A flat plate collector with an absorber surface area equal to the whole collector area or a tubular area with the absorber housed inside an evacuated glass tube is used for low- and medium-temperature water heating as well as space and industrial process heating. Concentrating collectors are utilized for high-temperature applications, which have benefits and disadvantages. The key benefit of a flat plate collector is better thermal efficiency, which results from the receiver's comparatively small area per unit of solar energy gathered, which greatly lowers heat loss and other expenses related to vacuum insulation and selective surface treatment. The

main downsides include the requirement for a tracking system and the ineffectiveness of collecting scattered radiation at a higher concentration ratio.

Concentrating solar collectors

Utilizing solar energy to address contemporary concerns including the depletion of fossil fuels, global warming, and population growth is one of the most viable solutions. Solar energy has a large exergy potential due to the sun's high temperature (approximately 5760 K) [1, 2]. A plentiful and sustainable source of energy is solar energy. As a result, a variety of uses requiring low to high temperatures may make use of solar energy. The following are the most frequent uses of solar energy, either as the only source of energy or in combination with other sources [3–5]:

The receiver and a concentrator are frequently used in concentrating collectors to help deliver large levels of solar irradiation to the receiver. Because of the concentration, the high-temperature operation is achievable, as well as a decrease in thermal losses owing to the receiver's tiny size. To keep thermal losses to a minimum at high operating temperatures, evacuated tubes are often employed as receivers. The non-concentrating type evacuated tube collector and flat plate collector cannot work at temperatures beyond 100 or 150° C; hence, concentrating technologies are employed instead. The concentrating collector's temperature is determined by its concentration ratio (C).

Non-imaging concentrating collectors have a concentration ratio of less than 5, and they often are utilized at temperatures up to 200 °C. Imaging concentrating collectors, on the other hand, have larger concentrations (typically over 10) and work at higher temperatures ranging between 200 and 500 °C. A greater concentration ratio allows for more efficient operation at higher temperatures. The following are the most common concentrating technologies:

- Concentrator with a compound parabolic shape (CPC), with concentration ratios ranging from 1 to 5, this is a concentrating collector of non-imaging type. This collector primarily uses sun beam irradiation, although a little degree of diffuse irradiation is also used, and the factor (1/C) is generally proportionate. The concentrator geometry is related to a large number of different designs. The receiver is normally tubular, and in applications requiring high temperatures, it is an evacuated tube collector. It depends on the CPC's design whether it can work with or without tracking. The system cost is lowered in the stationary mode, making it a financially viable option.
- The parabolic trough collector (PTC) is the most effective concentrating device among all which is used for industrial process heating and power generation purposes. It is a linear concentrating collector with temperatures ranging from 400 to 500 °C. The concentration ratio is commonly between 10 and 50, with ratios between 25 and 30 being more common. The PTC could work with a single-axis tracking system and, on rare occasions, a polar axis. Most of PTCs feature an evacuated tube receiver and uncovered or non-evacuated tubes are seldom used. The diameters of the absorbers range from 30 to 80 mm, with a typical value being 70 mm [6, 7].
- Similar to the PTC, the linear Fresnel reflector (LFR) operates in the same manner. The LFR, on the other hand, has fewer operating difficulties and lower wind loads in addition to being more affordable. Its optical performance, nevertheless, is worse than the PTC's. The concentration ratios of the LFR typically range from 10 to 400. In reality, the collection axis is aligned south to north and the LFR has a single-axis tracking mechanism. In addition to trapezoidal cavity designs, the receiver might be an evacuated tube collector with a secondary parabolic shape concentrator [8–11].
- In circular trough concentrators (CTC), solar flux non-uniformity is severe, so optical efficiency is highly dependent on the location and cross-sectional area of the receiver [12].
- Solar dish concentrators (SDC) are a focus-point technique with a high concentration ratio (around 100). These technologies are used for high-temperature applications, which may reach 600 °C and frequently integrate with solar tracking systems [13]. To analyze the thermal performance of a cylindrical cavity receiver used in a solar parabolic dish collector system, a thorough mathematical model, thermodynamic analysis, and optimization are carried out [14–16]. Dish collector systems with geometry modifications, with various flux conditions, weather conditions and different applications are investigated [17–19].
- Furthermore, it is crucial to note that although solar towers are vital in solar technologies, they are mostly employed for high-temperature power generation applications study.

Working principle of PTSC

Solar energy's utility for many purposes is limited by the fact that it is a cyclic time-dependent source of energy. As a result, solar systems need energy storage to supply power at night and during gloomy conditions. PTSC of PTC is a well-proven solar concentrating collector technique that can achieve temperatures of over 100°C and up to 450 °C. PTCs are used in a wide range of applications, including industrial

steam generation for power, industrial steam generation for process heat, and large-scale hot water community-level solar cooking.

A PTC [3, 20, 21] is a focused flat 1-D line with mirror surfaces with high reflectivity that bends like a parabolic in two dimensions. PTC's focus lane absorbs solar energy in the form of radiation along a path parallel to its equanimity plane, where concentrated solar radiation is collected using a pre-installed cylindrical tube absorber [17, 18].

A one-axis tracker might be built to ensure the solar concentrator and cylindrical tubular absorber function properly [22]. An ejected glass barrier is placed inside a metal tube covered with spectral lines to produce a cylindrical tubular absorber. To capture solar energy in its most concentrated form, an HTF (heat transfer fluid) such as liquefied salt, synthetic thermal oil, or even water flows into a cylindrical tubular absorber [23]. Micro-structured Ni–Cd is commonly used [24] to reduce long-wave emittance while increasing short-wave emittance. This suggests that the use of evacuated glass coverings and selective coatings can be used to reduce the heat losses encountered by cylindrical tubular absorbers [25]. To improve the optical efficiency of the system, a PTC with a cylindrical tubular absorber is used in a north–south orientation to track the Sun as it moves from dawn to midnight.

PTC with a cylindrical absorber might also be used in a dawn-to-dusk receiver direction, although this would diminish the system's photonic efficiency due to the loss of light. However, this could be handled by performing the needed PTC optimization using a cylindrical tubular absorber in response to changing weather conditions, obviating the requirement for tracing equipment. Using the described tracking mode would presumably assist achieve optimum efficiency during the fall and spring equinoxes while collecting very little radiation throughout the other seasons of the year. Continuous tracking of the Sun may sometimes generate inaccuracies that are lowest at midday and greatest at dawn and sunset. The concentration ratio at the same acceptance angle (107.3) is about one-third of the maximum value, which is for errors such as aiming error, surface error, and tracking error. The maximum value could be possible with more advanced concentrators that practically quadruple the concentration ratio and are based on secondary and primary designs that utilize anabolic optics [26–29]. Figure 1 shows a schematic of a parabolic trough collector.

Solar rays strike the receiver wall, which is angled in the direction of maximum radiation for maximum efficiency.

Figure 2 shows various industrial applications of a parabolic trough collector. Because the bulk of the preceding applications requires temperatures over 100 °C, flat plating processes cannot be used. As a result, concentrated solar collectors are employed in a variety of applications, and this study will concentrate on them. Current research on

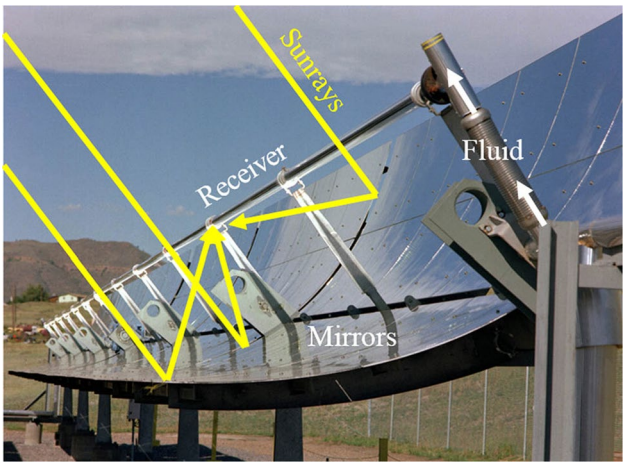

Fig. 1 Diagram of a parabolic trough solar collector [20]

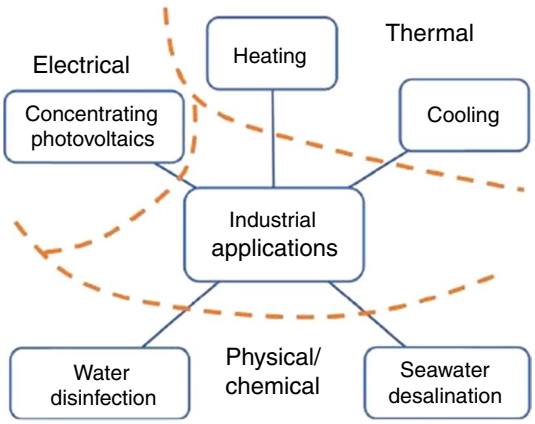

Fig. 2 Various industrial applications of parabolic trough collectors [20]

technological breakthroughs in concentrating collectors is emphasized, notably the use of nanofluids as working fluids in concentrating solar collectors.

An evacuated tubular receiver has a smaller optical performance in all types of trough reflectors than an open-aperture evacuated receiver, which avoids a dense distribution of reflected solar flux in a particular area of an absorber surface when exposed to high-density solar flux [12]. The thermal performance of a new type of solar water heater system consisting of an array of parabolic trough collectors and passive methods for thermal enhancements was studied [30–32].

Motivation and objectives

Utilizing solar energy to address contemporary concerns including the depletion of fossil fuels, global warming, and population growth is one of the most viable solutions. Solar energy has a large exergy potential due to the sun's high

temperature (approximately 5760 K) [33, 34]. A plentiful and sustainable source of energy is solar energy. As a result, a variety of uses requiring low to high temperatures may make use of solar energy. Frequent uses of solar energy either as the only source of energy or in combination with other sources are found [35–37].

Due to their large operating temperature range (between 100 and 700 °C) and potential for both power generation and industrial process heating, parabolic trough solar collectors (PTSCs) or parabolic trough collectors (PTCs) have attracted the attention of scientists and renewable energy enthusiasts. PTSC has been built in greater quantity than all other concentrated sun-producing apparatuses combined. The area for heat collecting sometimes referred to as the absorber tube and carrying fluids is one of the most crucial functional parts of the PTSC. Numerous studies on the fluids in the absorber tube flow have been done to boost its thermal potential. To enhance heat transfer and the system's overall effectiveness, better fluid thermo-physical characteristics are necessary. It was observed from the literature that an extensive review is needed to assess the suitable HTFs for PTSCs in specific applications. The current review aims to investigate various heat transfer fluids (HTF) that have been applied to PTSCs. Once-through kind PTSCs have a number of difficulties since two-phase flow is involved having water and steam as working fluid, which causes the tube to bend. Along with more traditional fluids like water and thermic fluid, the use of innovative HTFs such as nanofluids is also being studied. Hybrid nanofluids are also being researched for particular applications. Research on the manufacturing process, the stability of nanofluids, and the impact of hybrid nanofluids on PTSC thermal performance are all necessary. The section that follows covers specific working fluids in PTSCs for a variety of applications.

Working fluid used in absorber tubes of PTSC

Water/Steam

The thermal fluid most usually employed in solar thermal systems is water, which has a high heat capacity of 4.185 J kg^{-1} K^{-1} and is widely accessible. The only applications for solar thermal energy are for home and industrial process heating at temperatures between 70 and 250 °C. Demineralized water and a PTSC with a 90° rim angle and a concentration ratio value of 9.25 were used when operating at temperatures as high as 85 °C [21, 38]. The findings were compared to published values and it was discovered that the receiver was built to a high standard since the slope of the linear thermal efficiency equation, which takes thermal losses into account, was found to be 0.683. The investigation of the usage of parabolic trough collectors for food processing to generate steam has been elaborated [38]. Both the temperature of the produced steam and the outflow temperature of the solar field are gauged. The results demonstrated that a modest solar field may be used to generate enough steam using PTSC to meet the yearly steam requirement for the food processing industry. By doing this, you may save some land. Direct steam generation (DSG) provides a lot of advantages and few drawbacks. The usage of water during the phase shift enables a bigger mean temperature fall, a simpler plant structure, and higher temperatures near the solar field exit. In contrast to sensible heat transfer in molten salt and thermal oils, the required heat energy is absorbed during phase shift at low temperatures rather than at high temperatures, boosting thermal output and efficiency. Additionally, there is no environmental impact if water escapes onto the solar field because water is an environmentally safe substance [35]. Water requires less energy to remain liquid since its freezing point is lower than that of thermic oil or heat transfer fluid; even if it's lower than molten salts as well. In comparison with molten salts, water has a lesser propensity for corrosion [39]. The benefit of employing a steam-producing system with steam or water heat transfer is that it eliminates the need for a heat exchanger and the associated losses. We do draw attention to the fact that PTC generates high output temperatures, necessitating system design adjustments to avoid a rapid rise in water pressure caused by a temperature spike and boiling of the water. Even with the necessary feed water treatment, the absorber tube in this steam or water heat transfer system is susceptible to scaling. The scaling phenomena in multiple-row collector arrays may result in a loss of flow, which might degrade the selective receiver coating and induce tube dry-out. Thermal energy storage is hampered by the use of steam or water. Because the phase transition temperature is too low for the steam to expand in steam turbines and produce electricity, superheaters are employed to raise the temperature of the steam. Although the PTC can withstand temperatures of up to 500 °C, it cannot be utilized in applications that need lower temperatures and process heat since water is employed as the heat transfer fluid. PTSC having higher concentration ratio values provides more concentrated heat flux to generate electricity using a solar thermal-based power plan [21]. A heat transfer fluid with a greater operating temperature range is advised for applications that generate electricity. As will be discussed in more detail in the section after, synthetic oils, which can resist temperatures of up to 400 °C, are frequently employed in power plants.

Synthetic thermal oil

To avoid phase shift at high temperatures larger than 400 °C and high-pressure requirements, CSP power plants started using synthetic oil as HTF. The thermosol VP-1 is stable between 12 and 400 °C. When heated over its melting point, the hydrocarbon in this oil quickly degrades, releasing hydrogen gas. Makeup oil is required because of the degradation, which reduces the oil's shelf life. By-products from overheating the oil lead to the creation of sludge, which lowers thermal efficiency and increases plant maintenance costs [22]. Therminol D-12 was used as the primary HTF and water was used as the secondary HTF for quick heating in the methodology and calculation of Selvakumar et al. [40] concerning the parabolic trough collector performance. Over 100 cycles, the performance was examined. At 240 W m^{-2} and 540 W m^{-2}, the system generated hot water at 68 °C and 40 °C, respectively.

Efficiency is increased by 30% when Therminol D-12 and evacuated tubes are used in PTC instant hot water generating. We can determine how much synthetic oil can be used as HTF in PTC by looking at the working temperature range of the Therminol VP-1 (12–400 °C). A parabolic trough collector may operate at temperatures as high as 350 to 500 °C. The highest temperature at which a power plant can operate determines its efficiency. All of these properties allow Therminol VP-1 to be used as an HTF in PTC up to 400 °C. However, when the working temperature of the plant exceeds 400 °C, the synthetic oil starts to oxidize. High-temperature HTF can inhibit synthetic oil breakdown in high-temperature applications. When the temperature is high, molten salt therapy is a fantastic treatment for HTF. The section that follows discusses how molten salt is used in PTC applications.

Molten salts

In the seventeenth century, Humphery Davy [41] invented a method for extracting alkali metal from its hydroxide-fused salt. In nuclear reactors, molten salts were initially employed in the 1950s. The first molten salt reactor ever constructed, which was housed at Oak Ridge National Laboratory (ONRL), used thorium as the nuclear fuel. Molten salts are employed in CSP plants for heat storage and heat transmission reasons because of the rising concerns with environmental protection and renewable energy sources [42]. Figure 3 shows further uses for molten salts. Nitrate salts, which are the most often utilized molten salts in solar applications, have the potential to be exploited in heat transfer and thermal storage applications because of their unique chemical characteristics. Molten salts at high temperatures are desirable for their great density, low vapor pressure, promising specific heat, and exceptional stability at high temperatures. Because of their high specific heat capacities, which enable them to lower the size of the thermal storage tank, molten salts are more readily available, non-flammable, non-polluting, affordable, and environmentally friendly than synthetic oil. Due to the greater melting point of molten salt, which has various drawbacks, it is required to pre-heat and maintain the liquidus temperature at night.

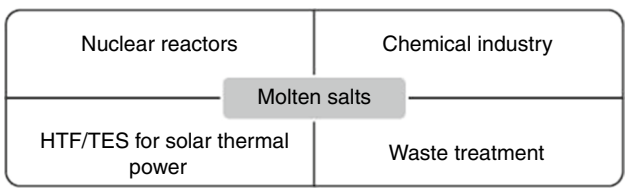

Fig. 3 Various molten salt applications [23]

The high running and maintenance expenses are a result of the energy needed to sustain this liquidus temperature. The features of the molten salts depend on their composition. Solar salt is the HTF most typically utilized in CSP systems. In their 3-D simulation of a PTSC using the computational fluid dynamics (CFD) model with solar salt as the heat transfer fluid, Wang et al. discovered that cross-sectional temperature rises with increasing direct normal irradiation and inflow velocity [43]. The key outcome of the study was that oil had a thermal efficiency of 573.15, which is 0.079 higher than that of molten salt at 773 K. Molten salt is used as the thermal energy storage component instead of synthetic thermal oil to reduce the cost of the heat transfer fluid (HTF). Solar salt is commonly used as reference material in research journals for TES and heat transfer applications [44]. Solar salt is produced at temperatures between 200 and 600°C. Because solar salt has a low melting point (222 °C), it may be utilized in CSP systems. To use PTC, the dynamic viscosity of the molten salt must be less than 0.005 Pa s since it requires more power to pump the fluid. At about 550 °C and 200 °C, respectively, Coscia et al. [45] molten salt had viscosities of 0.001 Pa s and 0.06 Pa s. Chen et al. [46] produced molten salt with a viscosity akin to water at temperatures exceeding 300 °C. The viscosity of the eutectic composite molten salt is significantly reduced by adding $Ca(NO_3)_2$ to solar salt. KNO_3:$NaNO_2$:$NaNO_3$ with mass fractions of 53%, 40%, and 7% make up the ternary eutectic combination known as HITEC. HITEC is thermally stable in the range of 142 to 535 °C. Numerous studies have looked at the HITEC molten salt's heat transmission properties and fluid flow parameters. Xiao et al. investigated the flow characteristics and heat transfer in a helical heat exchanger using HITEC as the working fluid on the hot side and DI water on the cold side [24]. They find that in both laminar and turbulent flow regimes, frictional pressure decreased.

The thermophysical characteristics of HITEC salt are shown in Fig. 4. The graph's trend indicates that HITEC

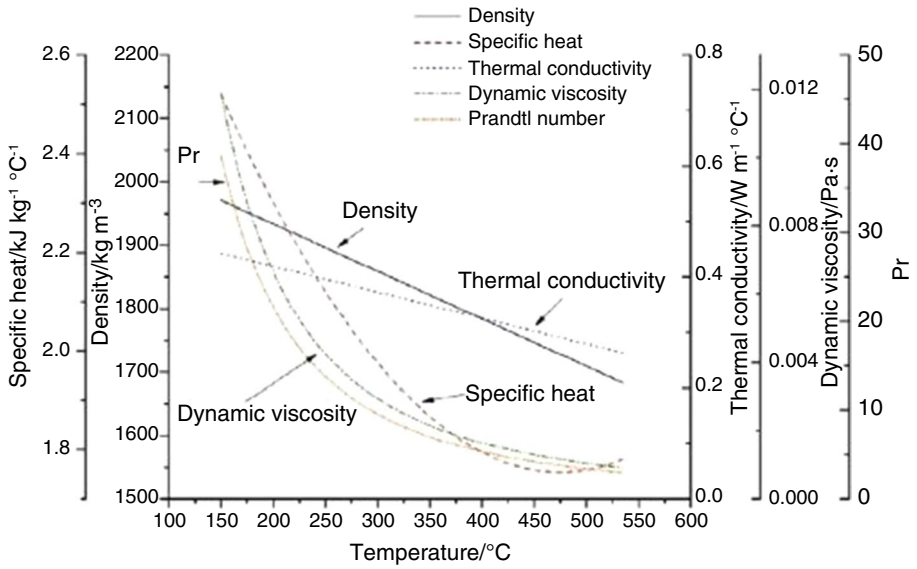

Fig. 4 Ternary nitrate molten salt thermophysical characteristics [24]

salt has high Prandtl values, or values above 7, even at low temperatures between 150 and 300 °C. Heat transport in the absorber tube is enhanced by the velocity boundary layer, which is substantially more significant than the thermal boundary layer with a larger Prandtl number. At temperatures between 300 and 500 °C, viscosity is greatly decreased. HITEC is a perfect working fluid for PTC since it operates within a comparable temperature range. In the ternary eutectic combination known as HITEC XL, KNO_3, $Ca(NO_3)_2$, and $NaNO_3$ have corresponding mass percentages of 43, 42, and 15%. Solar salt is transformed into HITEC XL molten salt by adding $Ca(NO_3)_2$ after the other components of the eutectic mixture. The thermal and physical properties of solar salt were studied by Fernandez et al., who discovered that adding calcium and lithium nitrate reduced the freezing temperature and the cost of the power plant [47]. These combinations were developed to lower the cost of utilizing synthetic oil as the working fluid and increase the heat storage capability of the parabolic trough collector system. Experimental observations supported the 3D molten temperature diagram. Chen et al. predicted for a combination of 42% KNO_3, 17% $NaNO_3$, and 41% Ca [46]. Chen and Zhao evaluated a particular HITEC XL composition ($Ca(NO_3)_2$ - $NaNO_3$ -KNO_3, 32:24:44 mass percent) and discovered that it had the highest performance, with a melting point of 80 °C and specific heats of 1.2 J g^{-1} $°C^{-1}$ for the liquid phase and 1.7 J g^{-1} $°C^{-1}$ for the solid phase, respectively [46]. Between 50 and 68 °C, where the curve is steady no matter how high the temperature increases, there is an increase in heat capacity. Because its specific heat capacity rises with temperature, liquid salt is sensitive to temperature changes. The combination has a thermal conductivity of 1–3 W/mK and almost zero

Table 1 Heat transfer fluid thermophysical characteristics appropriate for usage in PTC

Concentration of nanoparticles	Nanoparticles	Base fluid	Specific heat / kJ kg^{-1}		Augmentation %		Enthalpy / kJ kg^{-1}	Augmentation (%)	Reference
			Solid	Liquid	Solid	Liquid			
1 mass %	SiO_2	Li_2CO_3:K_2CO_3	–	1.365	–	10	–	–	[25]
0.125–0.15 mass %	Al_2O_3:MWCNT	Thermal Oil	–	–	–	–	–	–	[26]
1 mass %	SiO_2	KNO_3	1.224	1.203	9.5	6.1	102.46	12	[50]
1 mass %	Al_2O_3		1.068	1.043	− 4.5	− 7.8	92.10	0.5	
1 mass %	SiO_2–Al_2O_3		1.171	1.095	4.7	− 3.4	82.90	−9.5	
–	SiO_2	Li_2CO_3:K_2CO_3	–	2.05	–	27	–	–	[28]
	Al_2O_3		–	2.16	–	33	–	–	
	MgO		–	1.97	–	22	–	–	
32:24:44 mass %	–	$Ca(NO_3)_2$:$NaNO_3$:KNO_3	1.7	1.2	–	–	67	–	[51]
0.1 mass %	GNP	Water	–	3.849	–	−6.26	–	–	[52]
1 volume %	TiO_2	Diathermic oil	–	–	–	–	–	–	[53]
0.1–1 mass%	MWCNT	Thermal oil	–	–	–	–	–	–	[54]

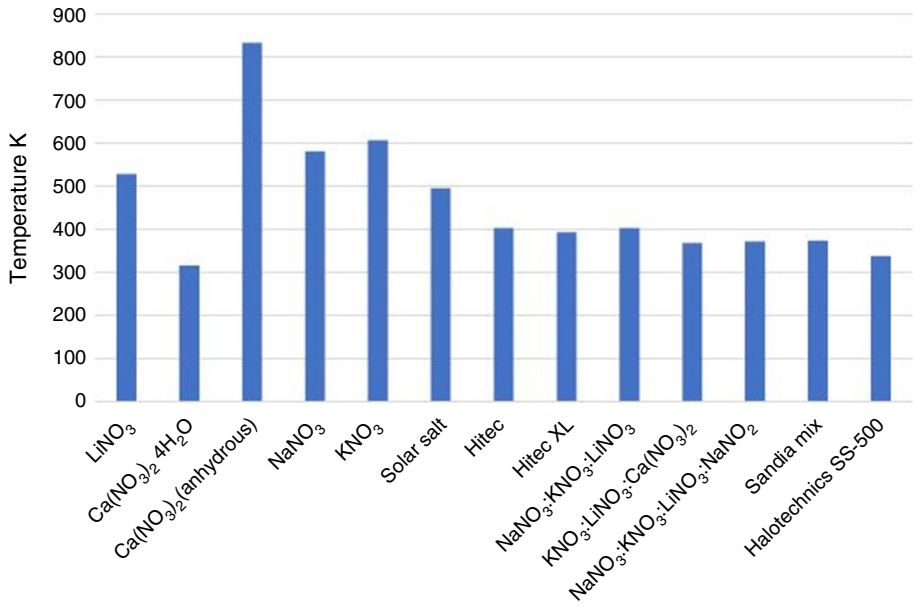

Fig. 5 Alkali salts melting points and their eutectic salts [48]

viscosity at 200 °C. Table 1 is a list of the thermophysical characteristics of HITEC XL. Due to its exceptional stability, high heat of fusion, and low cost, HITEC XL may be employed as a working fluid and a thermal energy storage material for line-focusing collectors. A ternary nitrate mixture's thermal stability was looked into by Fernandez et al. [47]. The thermal stability of solar salt and $LiNO_3$ salt-based eutectic composite was improved. The operational temperature range is between 130 and 600 °C, according to the study's findings. At 300 °C, the eutectic mixture forms a PTC salt and has a viscosity of 0.03 Pa s. The price of $LiNO_3$ ($4.32/kg) is the only disadvantage of this combo [48]. To develop a useful fluid and thermal energy storage medium, Zhao and Wu examined a eutectic combination of 50 to 80 mass percent KNO_3, 0 to 25 mass percent $LiNO_3$, and 10 to 45 mass percent $Ca(NO_3)_2$ [49].

According to the experimental results, this range of mass fractions is capable of achieving better viscosity, melting point, and high-temperature stability. Because of the eutectic mixture's high-temperature stability, the Rankine Cycle will operate more effectively [23].In PTC plants with HTF and TES, these special eutectic salts are therefore more adapted to replace synthetic oils. Quaternary eutectic salts of alkali nitrates and nitrites were investigated by Wang et al. as potential thermal liquids in a CSP [55]. The eutectic mixture's freezing point was determined to be roughly 100 °C based on differential scanning calorimeter data. The molten salt's temperature stability, which is lower than that of solar salt, Hitec, and HitecXL, is 430 °C. However, it seems that compared to solar salt and Hitec, salt has a higher specific heat capacity. At the Sandia National Laboratory, Bradshaw and Brosseau invented the novel molten salt known as "Sandia Mix" [34]. The study's focus was on the three unique mass ratios (QA, QB, and QC). Each exhibited thermal stability of more than 500 °C and a melting point of less than 100 °C. The composite mixture has a parabolic trough collector-appropriate viscosity of 0.003 Pa s. The price of $LiNO_3$ is Sandia Mix's major drawback in a commercial setting. By converting LiCO3 to HNO3, it could be cheaper to produce $LiNO_3$ salt on a large scale [56, 57].

Halotechnics SS-500 was created by Justin et al. [41] at Halotechnics Inc. utilizing the following ingredients: KNO_3 (23% mass percent), $LiNO_3$ (8% mass percent), CsNO3 (44% mass percent), $NaNO_3$ (6% mass percent), and $Ca(NO_3)_2$ (19% mass percent). Testing in nitrogen and air atmospheres revealed that the stability and melting point of this molten eutectic salt were up to 500 °C and 65 °C, respectively. Cesium-nitrate decreases the melting point of the molten salt mixture, however, compared to other molten salts, it is too expensive to be used in parabolic trough collector power plants. The mass ratio of CsNO3 is currently being improved by Halotechnics to lower expenses while maintaining a very low freezing point. HTF and TES have been effectively applied using molten salts. Low viscosity, a balance between specific heat capacity and thermal conductivity, a decreased melting point, and high-temperature stability are the main properties of molten salt developed for PTC application. The goal right now is to create an HTF that other academics may use as both a TES and an HTF. The melting points of several alkali salts and the matching eutectic compound are contrasted in Fig. 5. According to the literature, the melting point of the initial combination was lowered by adding $Ca(NO_3)_2$ and $LiNO_3$ to KNO_3 and $NaNO_3$, which led to the development of a eutectic mixture. By combining KNO_3, $Ca(NO_3)_2$, and $LiNO_3$, Coscia et al.

[45], Fernandez et al. [47], and Zhao et al. [49] created the eutectic mixture. When compared to salts that were separately melted, the results showed that $LiNO_3$ significantly lowered the freezing point. Chen et al. [46] discovered that the melting point decreased by 80 °C when $Ca(NO_3)_2$ was added to solar salt, which is in contrast to the melting point reduction patterns of another study, which range from 100 to 120 °C. The melting point could have been decreased by the researchers' preparatory procedures. Before mixing $Ca(NO_3)_2$ and $LiNO_3$ with solar salt, meticulous preparation is required due to the chemical's hygroscopic nature. The compounds must undergo several procedures to reduce their moisture content before they may be rendered anhydrous. When $Ca(NO_3)_2$ and $LiNO_3$ are mixed, the specific heat of the eutectic solar salt increases. According to Fernandez et al. [47], when $LiNO_3$ is added to solar salt, the specific heat increases. Zhao et al. [49] and Chen et al. [46] achieved the production of solar salt with about identical specific heat capacity using $Ca(NO_3)_2$. Molten salt must have a dynamic viscosity value of less than 0.005 Pa s to be used with PTC since viscosities greater than this need additional pumping force. At 550 °C, the viscosity of the molten salt produced by Coscia et al. [45] is 0.001 Pa s, while at 200 °C, it is 0.06 Pa s. Chen et al. found that the molten salt had a viscosity similar to water [46]. Numerous investigations have shown that the viscosity of the eutectic composite molten salt is significantly reduced by the addition of $LiNO_3$ and $Ca(NO_3)_2$ to solar salt. Therminol VP-1, water/steam, and solar salt were the three different HTFs that Montes et al. [43] investigated utilizing a parabolic trough collector loop with a 20 MWe power output. Energy efficiency decreases with length due to increasing heat loss throughout the whole receiver length. On the other hand, when both the output temperature and the energy efficiency increase, the trend is inverted. Exergy efficiency, however, declines as a result of the larger pressure drop caused by longer collector loops. Remember that for a given length of the receiver, molten salt and water/steam are more energy-efficient than the other two working fluids.

Gaseous heat transfer fluids

Using a gaseous working fluid is another approach to dealing with the need to operate at higher temperatures in PTC. The use of synthetic oil, water/steam, or molten salt as a heat transfer fluid in PTC has certain drawbacks [58].

To solve issues like high freezing points in molten salt, low thermal stability at high temperatures in synthetic oil, maintaining liquid water in a water-operated parabolic trough collector, high absorber tube corrosion caused by synthetic oil and molten salt, as well as poor environmental friendliness and cost-effectiveness, gaseous heat transfer fluids are used as the HTF in PTC. For instance, easily accessible non-toxic gases like neon, helium, nitrogen, and carbon dioxide are also fairly priced. Gases are employed in PTC to enable greater working temperatures, increasing the thermodynamic cycle's effectiveness [59]. Due to limitations like the heat transfer fluid's thermal stability, operational temperature corrosiveness, and environmental friendliness, the air is being utilized as a heat transfer fluid for the first time in a peak pilot-scale solar power plant in Ait Baha, Morocco. The facility generates 3.9 megawatts of thermal power and operates at a maximum temperature of 650 °C [58]. Regarding design elements, the PTC's collectors and receivers differ from those of conventional trough collectors. Biaxially oriented polyester sheets with a silvered top membrane are used to create collectors. An inflated ethylene tetrafluoroethylene (ETFE) membrane, as shown in Fig. 6, protects the absorber tube and receiver from the elements at the top. Additionally, Fig. 7 illustration of the absorber's cross-flow arrangement allows warmth to develop in each chamber. Because of this, the outlet and intake of the absorber are on the same side. A detailed thermodynamic study of a humidification and dehumidification (HDH) system using PTC and air as the HTF was performed by Fahad et al. [60]. PTC is placed between the humidifier and the dehumidifier in one system, and in front of the humidifier in the other. According to the study, the alternative technique offers a superior desalination plant structure and a higher gain output ratio (GOR). Carbon dioxide performs better than air at high temperatures. Additionally, carbon dioxide can transform into a supercritical fluid at 73.77 bar. Carbon dioxide is now denser and more thermally conductive than it was when it was a gas. Due to its properties, supercritical carbon dioxide is a superior HTF for PTC applications. The system's energy efficiency is increased by the enhanced thermal and hydrophobic properties of carbon dioxide in the supercritical state as opposed to its gaseous state [61]. Islam

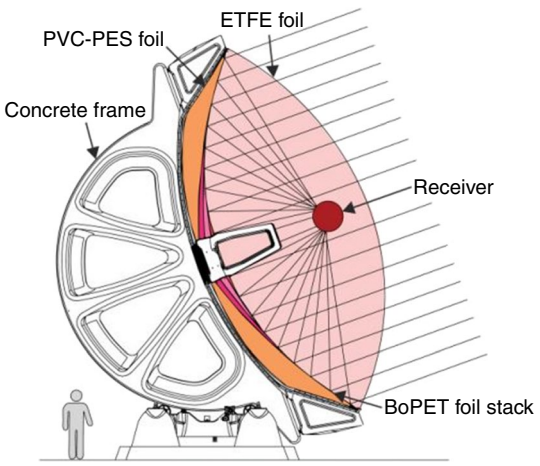

Fig. 6 Diagram of the solar collector used in Morocco power plant [58]

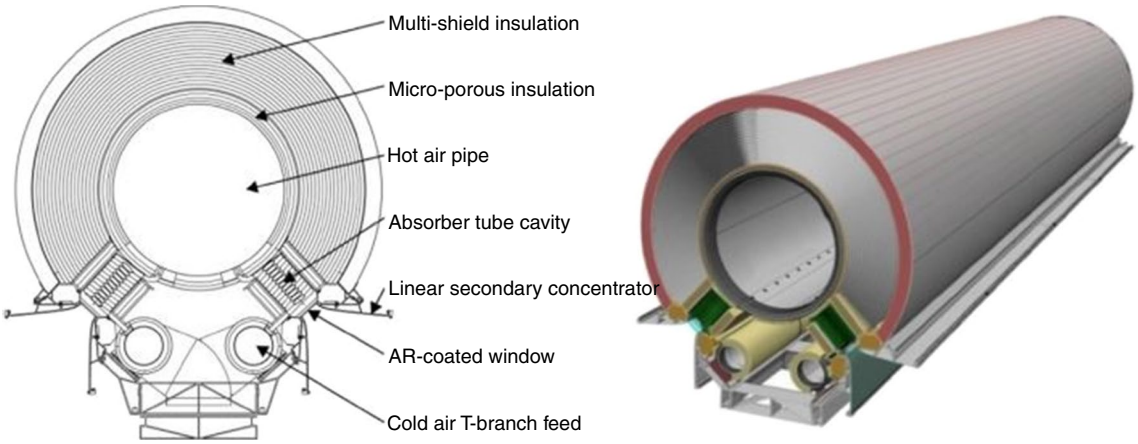

Fig. 7 Solar air receiver schematic cross section (left) and CAD image (right) [58]

et al. assessed the collector aperture area, heat removal factor, mass flow rate, and collector efficiency. Ammonia, nitrogen, and carbon dioxide were used as HTFs in the experiment. It has been discovered that the collector efficiency and heat removal factor are greatly influenced by the mass flow rate, collector aperture area, and collector concentration ratio [62]. The energy and exegetical behavior of carbon dioxide, argon, nitrogen, helium, and neon were studied by Bellos et al. They found that nitrogen operates similarly to air, with an energy efficiency of 0.4169, at 893 °C and a flow velocity of 0.15 kg s-1. The projected CO2 exergetic efficiency with a mass flow rate of 0.2 kg s-1 and an input temperature of 922 °C is 0.431. With an energetic efficiency of around 0.4338, helium has the greatest HTF among the examined gases, followed by neon and argon, with exergetic efficiencies of about 0.4047 and 0.3857, respectively. Due to its greater heat transfer efficiency and smaller pressure drop in the absorber, helium produced the most energy. The smallest gas is helium, which has an optimum temperature of 913 °C and a flow rate of around 0.0365 kg s-1. To guarantee the best energy efficiency, the maximum flow rates and input temperatures for argon and neon are set at 0.225 kg s-1 at 833 °C and 0.125 kg s-1 at 853 °C, respectively. As shown in Table 2, Bellos et al. computed the energy and exergy efficiency for various gases as well as the thermophysical characteristics of gaseous and other high-temperature HTFs [59]. HTF was looked at by Ravindra et al. for usage in CSP. They discovered that under collector conditions equivalent to those for liquid fluids, molten salt, and Hitec XL operating between 673 and 1150 °C, gaseous fluids required larger absorber tube diameters. In the 773–1150 °C temperature range, helium was shown to have a lower absorber tube diameter than CO2. CO2, on the other hand, has a greater benefit because of how commonplace it is in nature. Molten salt and helium perform better in terms of absorber tube length and heat transfer area. Over the entire operating temperature range, CO2 surpasses all gaseous and liquid HTF in terms of energy efficiency and effort. Table 3 [63] compares the physicochemical properties of liquid and gaseous HTF.

Liquid metals

In the thermo-nuclear industry, liquid metals have been employed for heat transfer applications. Liquid metals have recently been studied for their usage in solar applications. But, liquid metals have yet to be used in a commercial

Table 2 Energy and exergy efficiency of different gases utilized as heat transfer fluid in PTC [59]

Working fluid	$m_{optimum}$ / kg s^{-1})	$T_{in,Optimum}$ / K	Energy efficiency	Exergy efficiency	Convective heat transfer coefficient / W $m^{-2}K^{-1}$)	Change in pressure / kPa
Argon	0.225	560	0.6274	0.3857	100.6	10.22
Air	0.15	620	0.6459	0.4174	139.8	6.728
Neon	0.125	580	0.643	0.4047	130.2	7.598
Nitrogen	0.15	620	0.6475	0.4169	139.5	6.886
Helium	0.035	640	0.6631	0.4338	216.1	3.839
Carbon dioxide	0.2	660	0.6771	0.431	172.6	7.012

Table 3 Physical characteristics of liquid and gaseous heat transfer fluid are compared [63]

Working fluid	Flammability	Toxicity	Temperature limit for getting stable performance	Corrosivity
CO_2	Non-flammable	Non-toxic	Greater than 550 °C	Noncorrosive
Therminol VP1	Flammable	Toxic	Up to 400 °C	Corrosive
Helium	Non-flammable	Non-toxic	Greater than 550 °C	Noncorrosive
Dowtherm Q	Flammable	Toxic	Up to 400 °C	Noncorrosive
Hitec XL	Non-flammable	Non-toxic	Up to 550 °C	Low corrosivity

Table 4 Properties of liquid metals which are being researched for use in PTC [48]

Name	Melting Point / °C	Composition (in mass %)	Thermal Conductivity @ 600 °C / W m^{-1} K^{-1}	Specific heat capacity @ 600 °C /kJ kg^{-1} K^{-1}	Stability Limit / °C	Viscosity @ 600 °C / Pa s	Cost / \$ kg^{-1}
Na–K	− 12	Na:K:22.2:77.8	26.2	0.87	785	0.00018	2
Na	98	–	46.0	1.25	883	0.00021	2
Pb–Bi	125	Pb:Bi:44.5:55.5	12.8	0.15	1533	0.00108	13

parabolic trough power plant, despite their promising properties such as low viscosity, efficient heat transfer properties, and a broad working temperature range (98–883 °C) [49], which have attracted researchers' interest to the use of liquid metals in solar thermal engineering [30]. Important characteristics of liquid metals are listed in Table 4. Table 4 shows that liquid metals are more costly than HTFs made of water, air, molten salt, and oil. Additionally, liquid metals have a reduced specific heat capacity, which makes them a bad option for TES systems. In the next part, the research on using contemporary liquid metals as HTF in parabolic trough collectors is highlighted. Liquid sodium was employed as an HTF for the first time to power a 500 kW solar test facility in Almeria, Spain. Despite the sodium's successful performance, a fire at the testing site in 1986 forced its closure [64]. Table 4 lists the significant thermophysical characteristics of sodium. Compared to current-generation HTFs, sodium metal is more expensive and combustible when it comes into touch with moisture. These are the primary issues with it. Compared to other liquid metals, sodium is less corrosive when used with steel. However, a careful analysis of the corrosivity of liquid metals is required. Another HTF that is under investigation is the liquid metal eutectic Pb-Bi. 55.5% bismuth and 44.5% lead make up its eutectic composition. The term LBE is another name for the combo. The melting point of the molten salt employed in Hitec XL is 125 °C, which is also the melting point of this eutectic combination. LBE has a viscosity of 0.00108 Pa s, a specific heat capacity of 12.8, a thermal conductivity of 0.15, and a boiling point of 1533 °C at 600 °C [64]. The eutectic combination of Na–K, on the other hand, is a liquid metal that is the subject of investigation. It contains 77.8 mass percent potassium and 22.2 mass percent salt in a eutectic combination. These mixtures stand out because they can stay liquid at temperatures of 25 °C or below. Na–K has the advantage of being stable up to 785 °C and melting at 12 °C [48]. At 600 °C, the mixture's viscosity is 0.0 0 018 Pa s, its specific heat capacity is 0.87 kJ kg^{-1} K^{-1}, and its thermal conductivity is 26.2 W m^{-1} K^{-1}. The combination is four times more expensive than solar salt. Gallium metal that has been nano-enhanced with Al2O3 nanoparticles at concentrations of 5, 10, and 15% was examined by Sarafraz et al. At 200 °C, the generated gallium nanosuspensions were examined in microchannel blocks. As bulk Al2O3 concentration rose, the HTF's thermo-hydraulic performance decreased [65]. At lower heat flux levels, similar results were produced by doping liquid indium with copper oxide nanoparticles. The experiment aimed to investigate the effect of copper oxide doped indium as HTF on the heat transfer coefficient, pressure drop, and friction factor of the microchannel. The findings demonstrated that the heat transfer capabilities were not significantly enhanced by a decreased copper oxide content. The heat transfer coefficient dropped as the mass concentration increased, and the ideal thermal characteristics were found at 8 mass% mass concentration [65]. Liquid metals require more investigation to improve their qualities as compared to synthetic oil and molten salts as heat transfer fluids for parabolic trough collectors [48]. The right quantity of nanoparticles can improve the enthalpy, specific heat capacity, and corrosion resistance of liquid metals [65].

Ionic liquids

Thermal stability and a sizable thermal energy storage capacity are crucial for cost-effectiveness [66]. Ionic liquids (ILs) have a tremendous amount of promise as working fluids because of their remarkable thermo-physical properties, particularly for next-generation solar thermal collectors. The

unique characteristics of ILs, including their low volatility, ionic conductivity, thermal stability, and electrochemical stability, point to their application as a more advantageous substitute for volatile organic solvents [67]. The plethora of anions and cations gives the suggested ILs a wide range of properties. Oxazdium, imidazolium, triazolium, pyrazolium, thiazolium, pyridinium, pyrimidinium, pyridazinium, and pyrimidinium are among the organic cations and anions that make up the bulk of ILs. Viscosity restricts the application of IL. Although diminished heat stability may be a drawback of employing molecular solvents for viscosity reduction, this drawback may be overcome by using them. One of the practical possibilities for keeping the advantages of these materials seems to be combining ILs. Applications of the IL-ILs combination that have shown promise include gas solubilities, dye-sensitized solar cells, solvent reaction media, and stationary phases for gas chromatography. The class of molten salts known as ILs has a melting point below 100 °C and a maximum operating temperature of roughly 459 °C [55]. According to recent research, ILs lose some of their thermal stability between 200 and 250 °C [68]. Therminol VP-1 controls the collector field like how IL does. ILs are non-toxic, non-flammable, and non-hazardous and have a minimal impact on the environment when it comes to safety. Eck et al. forecast that IL would be inexpensive, but that the power block's efficiency will suffer due to its low working temperature. Due to this problem (low operating temperature), it is necessary to expand the collecting field, which surpasses the HTF's cost-effectiveness (IL). Paul et al. [66] evaluated the performance of this liquid, which was produced utilizing nanoparticles in parabolic trough collectors. Improvements in heat capacity of 49% and thermal conductivity of 11% were seen after using Al2O3 nanoparticles at a concentration ratio of 0.9 mass percent. In their investigations, Wittmar et al. [69] used surface-functionalized SiO2 in hydrophilic and hydrophobic imidazolium-based ionic liquids to generate theological performance and higher colloidal stability. The influences of gold nanoparticle surface state, particle size, and volume fraction were found to significantly boost the thermal conductivity of a stable ionic liquid-based nanofluid [70]. Four different ILs were utilized in Perissi et al. research of four ILs in contact with AISI 304 and 1080 steel sheets [71]. Since steel substrates in contact with various ILs still exhibit poor corrosion resistance at 220 °C—the working temperature of PTCs when used outdoors—they concluded that additional research is required. Ionic liquid/graphene nanofluids were investigated for high-temperature direct solar collectors and concentrated solar collectors by Jian Liu et al. [72] utilizing both experimental and computational techniques. They discovered that a 5 cm receiver operating at 20 kW m^2 could maintain a receiver efficiency of 0.7 at 600 K with a graphene concentration of 0.0005 mass percent.

Vegetable oil

Electrical industries, food processing, cutting oil for machining, HTF for heating and cooling purposes, and biodiesel for internal combustion engines, all require vegetable oil. Vegetable oil, on the other hand, is a viable option for applications demanding high temperatures owing to the depletion of fossil fuel stocks. Vegetable oil also exhibits thermophysical qualities similar to thermal oil, which is employed in solar power applications. Hoffmann et al. examined the thermal conductivity, density, and specific heat of copra, palm, soy bean, sunflower, rapeseed, and jatropha oils at temperatures ranging from room temperature to 250 °C. Rapeseed oil was found to have exceptional thermophysical characteristics, including dynamic viscosity, thermal conductivity, density, and specific heat, all of which were measured at 210 °C and had corresponding values of 3.2 m Pa s, 0.14 W m^{-1} K^{-1}, 788 kg m^{-3}, and 2.49 kJ kg^{-1} K^{-1}. Similar heat transfer properties were found for all seven vegetable oils. Due to their accessibility, affordability, biodegradability, and lower greenhouse gas emissions, vegetable oils are commonly utilized in solar parabolic trough collectors. Vegetable oils, on the other hand, are incredibly susceptible to oxidation. To improve their oxidation stability and offer meaningful remarks on their usage, more research is necessary [73].

Nanofluids and hybrid nanofluids

Preparation

Because it prevents instability and deposition, effective nanofluid preparation is critical for the improvement of thermal properties. On the production of a hybrid nanofluid, several investigations have been carried out by different researchers. The implications of nanofluid preparation are briefly covered here. The 1-step and 2-step approaches are the most prevalent nanofluid production techniques, as shown in Fig. 8 [74].

1-step method By sedimenting nanoparticles using a liquid-chemical method and a physical vapor deposition technique, a nanofluid is created in this operation. This method improved suspension stability while reducing particle aggregation.

This technique regulates the particle size distribution [75]. The pulse wire evaporation method was used in this operation to create nanofluid. The equipment included capacitors, a high-voltage gap switch, a high-voltage DC power supply, and a condensation chamber. Due to non-equilibrium heating, which results in wire evaporation and

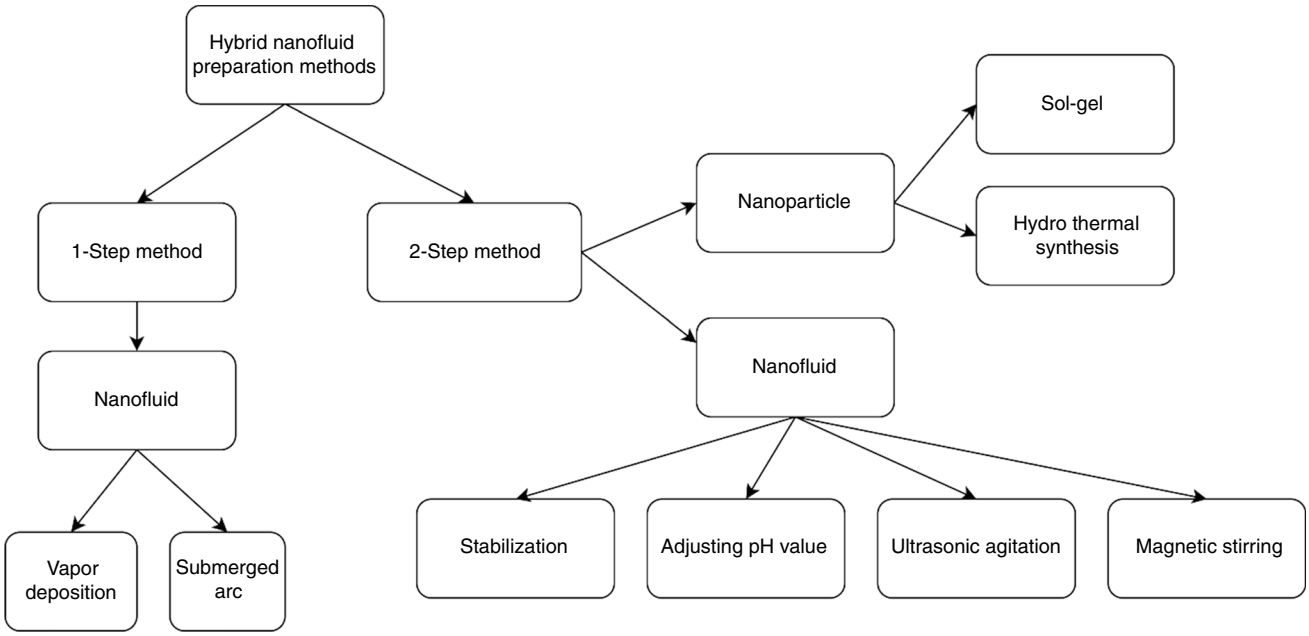

Fig. 8 Methods for creating hybrid nanofluids

conversion to plasma in a matter of microseconds, a high-voltage pulse of about 300 V is conveyed through a small wire. After that, inert gases like Ar and N2 are used to condense the plasma into a nanoscale powder. A hybrid nanofluid is created by concatenating a nanofluid with a certain volume concentration within an exploding bottle contained in a pulse wire evaporator. This hybrid nanofluid is then combined with the powdered nanoparticles discussed before.

2-step method The first step in this approach is to create dried, powdered nanoparticles. A thin dispersion of nanoparticles is added to the base fluid after the noble gases are evaporated, the solid sample is crushed, and the base fluid is then heated. Metal oxide does not develop when an inert gas is employed. When making metal oxide nanoparticles, oxygen is used in place of inert gas [76].

The fundamental drawback of this strategy is that it causes agglomeration, which leads to the deposition of sediments, as a result of strong Vander Wall forces that are stronger than the force. This prevents particle attraction from occurring before full dispersion in the fluid. Nanofluid exposure, ultrasonic waves, surfactants, and alterations have all been utilized to resolve this problem. Because metallic nanofluids must be oxidized, this process is cumbersome for their manufacture.

For large-scale and profitable manufacturing, a two-step process is best [77]. Chen et al. [78] used a two-step approach with a solution dodecyl-benzesulfonate surfactant to make

Table 5 Summary of methods for preparing hybrid nanofluids

Nanofluids	Shape of nanoparticles	Dimension of nanoparticles	Preparation method	Reference
Cu–Al/water	Spherical	$t_p = 10$ nm; $L_p = 46$–68 nm	1-step	[41]
Ag, Pd,Cu and Au/ethyl alcohol	Spherical	$D_{ps} = 5$–35 nm	1-step	[42]
Ag–MWCNTs/water	Spherical; cylindrical	D_p(Ag) = 80–90 nm; D_p(MWCNTs) = 20 nm; L_p (MWCNTs) = 5 µm	1-step	[43]
Cu–Zn–Al/water	Spherical	$t_p = 9$ nm; $L_p = 49$ nm	1-step	[44]
TiO_2–SiO_2/EG-water	Spherical	$D_{SiO2} = 22$ nm; $D_{TiO2} = 50$ nm	2-step	[45]
Al_2O_3–Cu/water	Spherical	$D_p = 15$ nm	2-step	[46]
Al_2O_3–Cu/EG and Al_2O_3/water	Spherical	$D_p = 10$–80 nm	2-step	[24]
Al_2O_3–Ag/water	Spherical	$D_p = 80$ nm	2-step	[47]

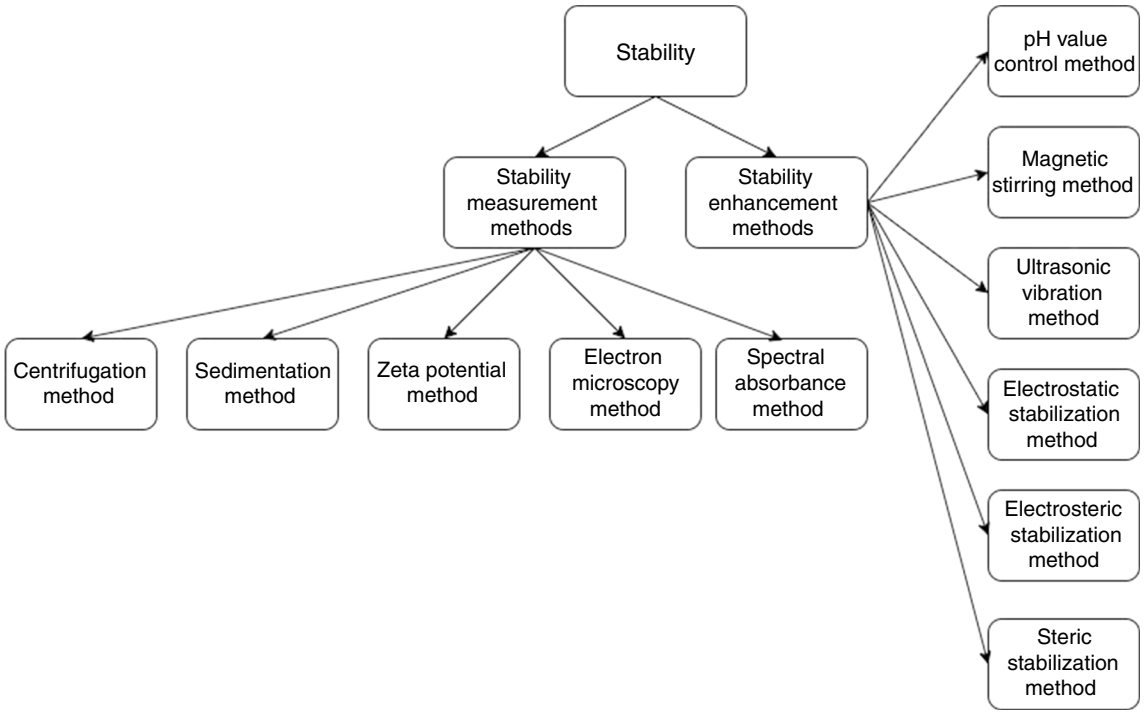

Fig. 9 Stability enhancement and measurement methods

the hybrid nanofluid (Fe_2O_3-MWCNT). Summary of methods for preparing hybrid nanofluids is presented in Table 5.

Stability

A hybrid nanofluid is defined as a liquid that has multiple kinds of nanoparticles scattered in it. Because of their high surface tension, nanoparticles quickly agglomerate together. This agglomeration process is responsible for the closing of ducts through which nanofluid flows, and particle settling, and; it also leads to the depreciation of the thermal properties of nanofluids [79]. Figure 9 shows the classification of hybrid nanofluid stability assessment and augmentation approaches. Making stable nanofluids is critical for determining the right values of thermophysical characteristics of nanofluids. An ultrasonic vibrator is the most common technique for creating a homogenized nanofluid.

Ultrasonication must be used frequently to prevent nanoparticle aggregation [80]. Various surfactants have been utilized to increase nanofluid stability by equally dispersing the nanoparticles in the base liquid.

Thermophysical properties

The thermophysical properties depend on how many nanoparticles are added to the basic liquids. Exact thermophysical property data are required to assess the thermal framework exhibition using hybrid nanofluids. Figure 10 displays several variables that influence the thermophysical characteristics of nanofluid.

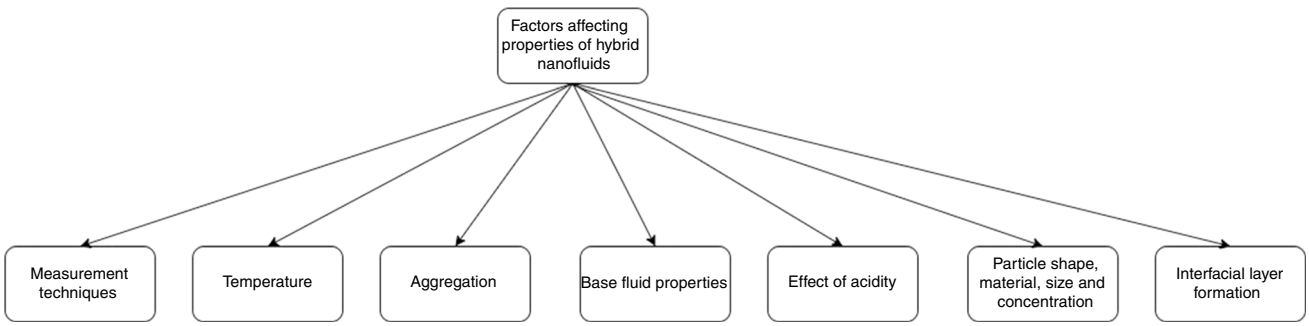

Fig. 10 Factors impacting the thermophysical characteristics of hybrid nanofluids

These thermal liquids' properties include viscosity, density, specific heat, thermal conductivity, and others. The pressure drop and heat transfer coefficient are two more important considerations. Based on physical factors such as surfactant, nanoparticle size and shape, and volume concentration, these properties may be described. Without taking into account the pressure drop, flow, and pumping power that occurs during nanoparticle motion in a liquid environment, the thermal conductivity of liquids is exactly proportional to their capacity for heat transfer [81]. The size, shape, and type of nanoparticles have an impact on the hybrid nanofluids' thermal conductivity. Compared to nanofluids containing spherical nanoparticles, barrel-shaped nanoparticles (also known as tubes or nanorods) have a higher thermal conductivity.

Additionally, thermal conductivity is improved in small-particle nanofluids over larger ones. According to the study [82], metallic nanoparticles have superior thermal conductivity than non-metallic (oxide) nanoparticles. The hybrid nanofluid thickens as the particle volume concentration of nanocomposites increases. The concentration of the hybrid nanofluid increases along with the predicted viscosity. Particle size, volume fraction, size, solution pH estimates, surfactants, base fluid ionic quality, particle surface nature, Vander Walls attractive forces, and double-layered repulsive forces are a few variables that affect the viscosity of nanofluids [83].

Surfactant addition to nanofluids must be carefully controlled, as too much will have a negative impact on the nanofluids' thermal properties, chemical stability, and viscosity. Meanwhile, nanoparticles in the base liquids aid in the formation of the cluster and speed up the adsorption process on the surface. These variables also induced a considerable increase in viscosity by increasing the hydrodynamic distance between nanoparticles [84]. When evaluating the thermophysical qualities, a few factors should be taken into account, such as the working temperature, and base fluid [85].

Thermal conductivity When two or more different types of nanoparticles are introduced to the base fluid to increase the nanofluid's thermal conductivity, the hybrid nanofluid performs better than the single particle or mono nanofluid [86]. The size of the nanoparticles significantly affects the thermal conductivity of nanofluids. The impact of particle size on the thermal conductivity of nanofluids has not been considered by researchers. Nanofluids' increased heat conductivity is a result of their smaller particle size. Cylindrical and spherical nanoparticles are used to explore nanofluids. The thermal conductivity of cylindrical particles increases over time [87]. Temperature affects the thermal conductivity of nanofluids. Nanofluids' thermal conductivity rises as the temperature rises. Nonetheless, to improve thermal conductivity, a considerable amount of surfactants or chemical solvents should be added to the nanofluid [88]. An overview of thermal conductivity of different hybrid nanofluids is presented in Table 6.

Viscosity Viscosity is the ability of a fluid to resist deforming when sheared or squeezed lengthwise. Newtonian and non-Newtonian fluids are the two categories into which fluids fall.

A Newtonian fluid's shear stress reflects the change in shear rate, while a non-Newtonian fluid's viscosity does not under conditions of constant pressure and temperature [91]. Due to the suspension structure of the nanofluid, which has obvious implications for convection pressure drop, viscosity plays a specific role in the framework's design [92]. Therefore, before they can be employed in a variety of applications, the increase in the viscosity of nanofluids in contrast to their base fluid needs to be carefully examined and analyzed. Nanofluids often have a greater viscosity than their fundamental fluids [93]. The key factor becomes even more obvious as the nanoparticle volume concentration rises.

Additionally, the bulk of scientists has studied how nanoparticles affect the viscosity of nanofluids. It is important to take into account the impact of several variables on viscosity, including the type, size, and condition of nano-added compounds, base fluids, and temperature [94]. Hybrid nanofluids offer greater heat transmission than regular fluids in the vast majority of situations, despite their high viscosity. One of the most economical and mild methods for heat transmission in heat exchangers is the use of high-thermal-conductivity materials scattered in the base fluid. Viscosity is improved by varying nanoparticle sizes and increasing volume concentration (Table 7).

Specific heat capacity and density The size of scattered nanoparticles has an impact on hybrid nanofluids' specific heat as well. Smaller nanoparticles have an increasing specific heat compared to bigger ones. A reduction in specific heat was seen as particle size increased [95]. Since smaller particles have more surface atoms than larger ones, their specific heat should be greater. Therefore, smaller particles with a higher heat capacity are suitable [96]. Riazi et al. [97] used a differential scanning calorimeter (DSC) to detect specific heat. The density of the nanofluid increased along with the volume concentration inside the base fluid as temperature increased. This happened when the density of the hybrid nanofluid was taken into consideration. When the base fluid's nanoparticle density is off, agglomeration happens, completely disrupting the stability of the nanofluid [98]. A density meter is necessary to determine the densities of various hybrid nanofluid types (DMA 5000). The mass-spring model is used to establish the estimated standard [99]. An overview of density and specific heat of different hybrid nanofluids are presented in Table 8, and 9 respectively.

Table 6 An overview of the thermal conductivity of several hybrid nanofluids

Nanofluids	Size of nanoparticles	Volume concentration	Thermal conductivity enhancement	References
Fe_3O_4–CNTs/DI water	D_p = 10–30 nm	Fe_3O_4 = 0.1–0.9%; CNTs = 0.05–1.35%;	44.6% at 55 °C	[57]
Zn–Fe_2O_4/water	D_{Fe2O4} = 20 nm; D_{Zn} = 2 nm	0.5%	11.8% at 30–80 °C	[25]
Al_2O_3–Cu (50:50)/EG	D_p (Cu) = 70 nm; D_p(Al_2O_3) = 5 nm;	0.125–2.0%	28% at 50 °C	[26]
Al_2O_3–MWCNTs (85:15)/thermal oil	D_p (MWCNTs) = 20–30 nm; D_p (Al_2O_3) = 20 nm	0.125–1.5%	45% at 50 °C	[50]
Cu–TiO_2/water	D_p (Cu–TiO_2) = 55 nm	0.1–2.0%	2% at 90 °C	[28]
SiC–TiO_2/diathermic oil	D_p(TiO_2) = 10 nm; D_p (SiC) = 30 nm	0.1–1.0%	8.39% at 43 °C	[51]
MgO–f–MWCNTs/EG	D_p (f-MWCNTs) = 5–15 nm; D_p (MgO) = 40 nm	0–0.6%	21.3% at 25 °C	[52]
ZnO–TiO_2/EG	D_p (TiO_2) = 30 nm; D_p (ZnO) = 35–45 nm	0.1–3.5%	32% at 50 °C	[53]
ZnO–Ag/water	D_p (Ag) = 30–50 nm; D_p (ZnO) = 10–30 nm	0.125–2.0%	26% at 50 °C	[54]
CNTs–Al_2O_3/water	D_p (Al_2O_3) = 20 nm; D_p(CNTs) = 5 nm–15 nm	0.02–1.0%	15% at 59 °C	[89]
Graphene nanoplatelets–Platinum/water	Nanoplatelets = 2 mm	0.02–0.1%	17.77% at 40 °C	[58]
FMWCNTs–Fe_3O_4/EG	D_p (f-MWCNTs) = 5–15 nm; D_p(Fe_3O_4) = 20–30 nm	0–2.3%	30% at 50 °C	[59]
Ag–MWCNTs/water	D_p (Ag) = 30 nm; D_p (MCNTs) = 10 nm	0.1%	20.4% at 40 °C	[60]
TiO_2–CNTs/water	D_p (TiO_2) = 22–32 nm; D_p (CNTs) < 8 nm	0.1–0.2%	20.5% at 25 °C	[61]
CNTs–Fe_3O_4/water	D_p (CNTs) = 10–30 nm	0.1–0.3%	28.46% at 60 °C	[62]
SiO_2–graphene/naphthenic mineral oil	Graphene = 12 nm	.01–0.08%	80% at 100 °C	[63]
Co_3O_4–GO/water	D_p (Co_3O_4–GO) = 50 nm	0.05–0.2%	19.14% at 60 °C	[90]
Al_2O_3–CuO/water and EG	D_p (Al_2O_3) = 20 nm; D_p (CuO) = 14 nm–20 nm	0.05–0.2%	45% at 70 °C	[64]
WO_3–Ag/Transformer oil	D_p (WO_3) = 60 nm	1.0–4.0%	41% at 100 °C	[65]
MWCNTS-HEG/DI water, EG	D_p (MWCNTs) = 30 nm–40 nm	0.04–0.08%	80% at 50 °C	[66]
SWCNTs–Al_2O_3 (30:70)/EG	D_p (Al_2O_3) = 20 nm; D_p (SWCNTs) = 1 nm–2 nm	0.04–2.5%	41.2% at 50 °C	[67]
Cu–TiO_2/water and EG (60:40)	D_p (TiO_2) = 40 nm; D_p (Cu) = 70 nm	0.1–2.0%	42% at 60 °C	[68]
SWCNTs–CuO/water and EG (60:40)	D_p (CuO) = 40 nm; D_p (SWCNTs) = 2 nm	.02–0.75%	36.2% at 50 °C	[69]

Table 7 An overview of the viscosity of several hybrid nanofluids

Nanofluids	Size of nanoparticles	Volume concentration (%)	Viscosity enhancement (%)	References
ZnO–MWCNTs/engine oil	D_p = 30 nm	0.125–1.0	45	[70]
SiO_2–MWCNTs/SAE40 oil	D_{MWCNTs} = 5–15 nm; D_{SiO2} = 20–30 nm; and L_{MWCNTs} = 50 µm	0–1.0	37.4	[71]
Ag–Fe_3O_4/EG	D_{Fe3O4} = 20–30 nm and D_{Ag} = 30–50 nm	0.3	42.8	[72]
SiO_2–MWCNTs/water–EG	D_{MWCNTs} = 5–15 nm; D_{SiO2} = 20–30 nm; and L_{MWCNTs} = 50 µm	0.0625–2.0	2	[73]
MWCNTs–MgO/EG	D_{MWCNTs} = 10–30 nm; D_{MgO} = 40 nm; and L_{MWCNTs} = 10 µm	0.0625–1	20	[74]
MgO–MWCNTs/EG	D_{MWCNTs} = 5–20 nm and D_{MgO} = 40 nm	0–1	168	[75]
CNTs–Fe_3O_4/water	D_{CNTs} = 10–30 nm; D_{Fe3O4} = 20–30 nm and L_{CNTs} = 10 µm	0.1–0.9	59.09	[76]
MWCNTs–SiO_2 (20:80)/20W50	D_{MWCNTs} = 20 nm and D_{SiO2} = 40 nm	0.05–1	171	[77]
MWCNTs–MgO (20:80)/SAE50	D_p = 30 nm	0.025–2	65	[78]
MgO–MWCNTs/water and EG (60:40)	D_{MWCNTs} = 5–15 nm and D_{MgO} = 40 nm	0.025–0.8	43.47	[79]

Table 8 An overview of the density of several hybrid nanofluids

Nanofluids	Size of nanoparticles	Nanoparticles mass/volume fraction	Density	Reference
Graphene oxide (GO)- Co_3O_4/water	$D_{GO–Co3O4} = 100$ nm	0.05–0.15%	$\rho = 4.45\%$ (↑)	[90]
AgeMgO/water	$D_{Ag} = 25$ nm; $D_{MgO} = 40$ nm	1.5–2.0%	$\rho = 9.59\%$ (↑)	[68]
GNP–Ag/water	$D_{GNP} = 2$ µm	0.02–0.1 mass%	$\rho = 0.14\%$ (↑)	[80]
Al_2O_3–Cu/water	$(Al_2O_3:Cu)_{powder} = 90:10$	0.1 vol%; 1.0 vol%	$\rho = 1.74\%$ (↑)	[81]

Table 9 An overview of the specific heat of several hybrid nanofluids

Nanofluids	Size of nanoparticles	Nanoparticles mass/volume fraction	Specific heat	Reference
Al_2O_3–Si_2O_3/water	$D_{Si2O3} = 20$ nm and $D_{Al2O3} = 45$ nm	0–3%	$C_p = 18.38\%$ (↓)	[82]
Al_2O_3–ZnO/water	$D_{ZnO} = 70$ nm and $D_{Al2O3} = 29$ nm	0.33–1.67%	$C_p = 30.12\%$ (↓)	[83]
SiO_2–Al_2O_3/$NaNO_3$–KNO_3 (60:40)	$D_{SiO2–Al2O3} = 2$–200 nm	.5–1.5 mass%	$C_p = 22.5\%$ (↑) at liquid phase and $C_p = 57.7\%$ (↑) at solid phase	[84]
Al_2O_3–MEPCM/water	MEPCM = 4–10 µm	0–3%	$C_p = 13.17\%$ (↓)	[85]
rGO–Co_3O_4/water	–	0.05–0.2 mass%	$C_p = 0.17\%$ (↓)	[86]
Al_2O_3–CuO/water and EG	$D_{CuO} = 24$ nm and $D_{Al2O3} = 8$ nm	0–0.6%	$C_p = 26.22\%$ (↓)	[87]

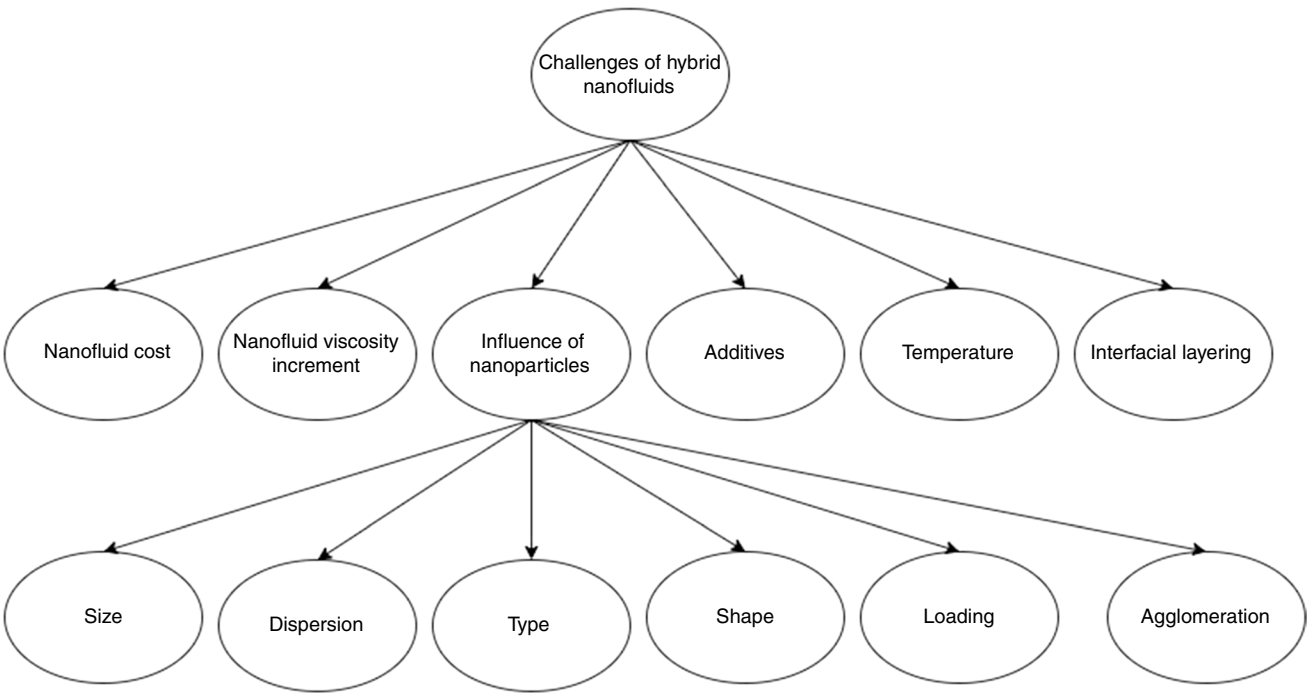

Fig. 11 Challenges of hybrid nanofluids

Challenges and their impact on performance

Hybrid nanofluids are novel fluids that are now undergoing testing and are being adequately accounted for with acceptable heat transfer, but they still have many obstacles to overcome (as shown in Fig. 11) before being used and incorporated. There are several discrepancies between exploratory findings, speculative projections, and actual information for a hybrid nanofluid [76]. The stability of nanocomposite nanoparticles in the base fluid is one of the major issues in nanofluids. As a result, consideration should be paid to the following considerations while creating hybrid nanofluids [100]:

A mixture of nanocomposite materials.

The selection of suitable materials.

A sufficient amount of surfactant is used.

Binding between the many nanoparticles that make up the composite.

The cost of these nanoparticles is also a problem.

As a result, the goal is to reduce costs while increasing the efficiency of their commercialization initiatives [76]. In comparison with the base fluid, the hybrid nanofluids have a severe deficit in terms of viscosity enhancement. When used in an inward cascade, nanofluids cause a pressure drop to increase, increasing pumping power [84]. Figure 10 depicts many performance-impacting characteristics.

Foam formation It is difficult to get a stable nanofluid since hybrid nanoparticles have a hydrophobic propensity. As a result, particles will be unusually gathered at the air/water boundary and watery stage, and stable air pockets may be produced under appropriate circumstances [101]. Foam's viscosity may be fundamentally enlarged due to the proximity of air pockets, leading the resultant fluids to clear poor penetrability locations [102]. Foaming agents are also utilized to improve microscopic uprooting efficacy.

The oil–water surface tension will be reduced by these substances [103]. The use of nanoparticles and polymeric elements to improve foam stability is highly recommended. Figure 12 depicts several foam formation removal strategies.

Stability Stability is a key strain that impairs system performance and renders good results undesirable. Any hybrid nanofluid that wants to improve its thermal properties must be in a stable phase. To achieve this stability, hybrid nanoparticles are adequately disseminated in the basic fluids. As a result, the stability gave rise to several problems or confronted professionals with new problems [104]. Stable hybrid nanofluids have been created via a variety of physical or synthetic processes, including surfactant application, strong force application on clusters of nanoparticles, and surface modification of nanoparticles. Various dispersion agents are utilized to obtain properly distributed hydrophobic nanoparticles into the fluid [105]. Some of the flaws that

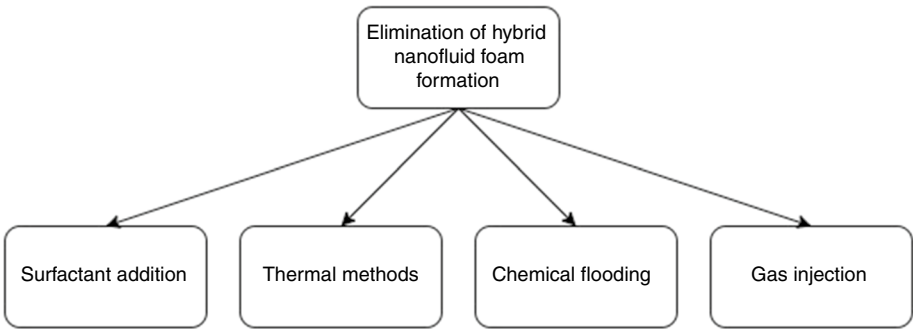

Fig. 12 Methods for preventing hybrid nanofluids foam formation

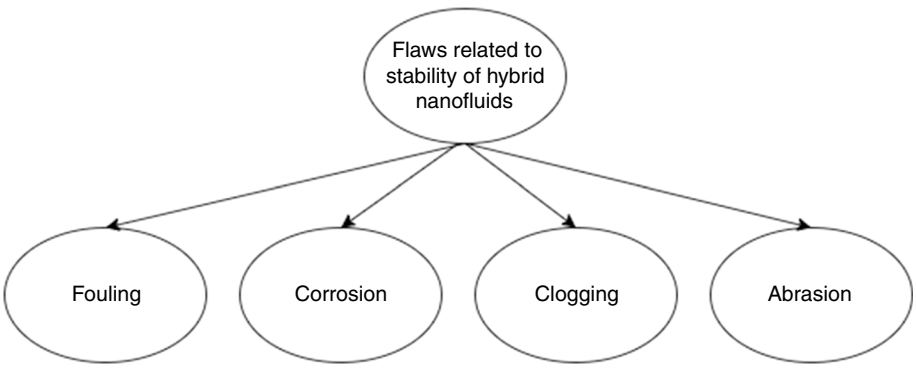

Fig. 13 Hybrid nanofluids stability flaws

are related to the stability of these types of fluids are shown in Fig. 13.

Production cost The challenge is to supply large volumes of hybrid nanofluids with low effort. These fluids have not been scaled up to large-scale production. Nanofluids are not preferred by several small-scale enterprises due to their high cost. The price will remain high until nanofluid synthesis allows for greater hybrid nanoparticle formation [101]. Nanofluid is synthesized using single-step or two-step processes. In any case, both strategies need sophisticated systems [105]. The price-performance factor (PPF) of a nanofluid is determined by the ratio of the nanofluid's thermal conductivity to that of the base fluid and by the cost of the nanofluid. When the thermal conductivity percentage decreases as a result of molecular aggregation, sedimentation, or deposition, a price performance factor expires. The cost of manufacture is higher, and the thermal conductivity ratio is higher for nanofluids with smaller molecular sizes. The cost of the nanoparticle material has an impact on the price of the nanofluid; for example, metal and carbon-based nanoparticles are expensive, but production costs for metal oxide-based nanofluid are lower. The relationship between price and performance is described as follows[106].

Pumping power Increased thermal and exergy productivity may be achieved by increasing the number of nanoparticles in nanofluids. In any event, this might result in a bigger pressure drop, which could increase the pumping power of the system [107]. An Al_2O_3/synthetic oil nanofluid with a 13 nm size was studied by Ferraro et al. [86]. The analysis found that neither the pressure drop nor the thermal efficiency had significantly increased. The use of nanofluid resulted in lower pumping power needs [108]. The research was done on an 8% volume concentration of Al2O3/synthetic oil nanofluid. The researchers found that higher pumping power is needed when the volume concentration of nanofluid approaches 4%. A key difficulty with hybrid nanofluids is an inevitable rise in friction factor. The friction factor, which necessitates a lot of pumping power, reduces the heat transfer capabilities of hybrid nanofluids [109]. Sundar et al. [110] investigated Fe_3O_4- MWCNT/water in their research. The data revealed that when Re 14 22,000 is used, the friction factor increases by 1.18 times. Biswas et al. [111] investigated the pumping power of a porous cavity using a Cu/water nanofluid. Nanofluid needs greater pumping power than base fluid, according to the study. The use of nanofluid resulted in an 18% increase in pumping power. Rahmanian and Hamzavi [112] investigated the pumping power effect in a thermal system utilizing a CNT nanofluid. An increase in pumping power resulted in a 0.92% decrease in electrical efficiency, according to the research. The friction factor increased due to the abrasiveness of the dispersed particles against the channel walls.

Proper selection of hybrid nanomaterials and base fluid Correct selection of the production technique and suitable hybrid nanoparticles is required for the synthesis of diverse nanoparticles. Below are some factors to consider for the optimal selection of hybrid nanomaterials and base fluid [113]:

Optimized nanofluid evaluation in terms of size, type, particle shape, temperature, nanofluid stability, and production procedures. The proper ratio of nanoparticles to base fluid should be determined to get the highest significant heat conductivity as well as the lowest feasible viscosity. This is necessary to lower the system's pressure drop and to satisfy the demands of heat transmission. The choice of the optimal pH value for nanofluids is important because it affects the dependability and thermophysical characteristics of nanofluids. According to the studies described above, the effective selection of base fluid and hybrid nanomaterials is a major difficulty for researchers to overcome in future investigations.

Nanofluids and advantages The main goals of industrial applications are to reduce production time, extend the life of equipment, and save energy, all of which may be accomplished by increasing the heat transfer rate. The total performance of an energy system is reduced because of the limited thermal conductivity of conventional working fluids like water, oils, and other similar substances. As a result, a great deal of study has been done to solve this issue. The usage of nanofluids is a viable method for enhancing performance. The presence of nanoparticles improves the system's efficacy by reducing the thickness of the thermal boundary layer and increasing the fluid's thermal conductivity plus the heat transfer rate. In traditional fluids, solid nanoparticles (1–100 nm) are present in nanofluids. Solid nanoparticles (1–100 nm) are found in nanofluids, as they are in regular fluids [114]. An increase in viscosity and, as a result, a decrease in Reynolds number are caused by an increase in nanofluid particle concentration. Furthermore, it reduces the heat capacity of the fluid, making it more conductive. As a result, the Prandtl number lowers and the thermal diffusion rate rises. Nusselt number falls in the end since it is dependent on Reynolds and Prandtl numbers. However, when particle size increases, the Nusselt number increases, and heat conductivity drops [115]. The use of nanofluids has a few drawbacks, such as mixing instability and expensive prices.

Cu, CuO, Al_2O_3, TiO_2, Fe_3O_4, SiC, CNT, Ag, Au, Ni, and other nanoparticles have been used extensively in research. Several experiments using passive techniques

and the usage of nanofluids have been conducted in recent years.

The influence of thermal oil, water, and ethylene glycol, as well as two nanofluids, TiO_2–H_2O and CuO–H_2O on an absorber tube with a triangular cross section and with forwarding perforated ring steps was investigated by Mahmoudi et al. [116]. The influence of the step distance, step inner diameter, working fluid, and nanoparticle volume concentration was all investigated. When flowing through a tube with inserts, and using a 4% particle concentration in CuO-H_2O nanofluid, the maximum thermal efficiency ranged from 67 to 76.5%. The value of efficiency for tubes operating with water as working fluid and equipped with inserts ranged from 66 to 73%. Gnielinski correlation was used to verify the numerical model.

Rostami et al. [117] used Cu/SBA-15 hybrid nanofluid to determine the exergy and energy efficiency of an absorber tube using turbulators as inserts. The heat transfer improvement is minimal for low Reynolds numbers (less than 3500), according to the CFD analysis. After that, the average Nu rises in contrast to a smooth absorber tube.

During the noontime hours, the maximum energy and exergy efficiencies were determined to be 65% and 5%, respectively, which were 2% and 1% higher than the ordinary scenario. Bilal et al. [118] investigated and experimentally confirmed the linked effect of Fe_3O_4–H_2O nanofluid and twisted tape inserts.

The results show that when compared to a smooth absorber tube, water with insert, tubes with nanofluid, and nanofluid with insert had maximum enhancements of 59%, 56%, and 63% to 87%, respectively, validating the usage of nanofluid within the absorber tube. When tubes were filled with nanofluid or twisted tape, however, effective thermal efficiency was found to be similar.

Hatami et al. [119] used FlexPDE software to conduct a FEM-based assessment to investigate the effects of various nanoparticles and absorber tube porosity. The absorber tube was made semicircular by filling it with a porous material. Under uniform heat flow conditions, the influence of nanofluid types, volume fractions, Rayleigh numbers, and Darcy numbers on the enhancement of heat transfer was examined. Cu, Al_2O_3, Fe_3O_4, and TiO_2 were among the water-based nanofluids utilized. Cu-based nanofluid has the highest average Nusselt number of 4.5 due to its increased thermal conductivity.

Using Dowtherm-A as the base fluid and four distinct nanoparticles (Al_2O_3, SiC, C, and Cu) when fed through a receiver tube with longitudinal fins, Benabderrahmane et al. [120] studied the impact of various nanoparticles in thermal oil (in two different sizes with triangular and rectangular cross sections). The friction factor and Nusselt number increased by 1.6 to 1.85 and 1.3 to 1.8 times, respectively, when the insert's results were compared to those of a smooth tube. Additionally, using insert and Cu-based nanofluid together produced an enhancement factor of 1.3 to 1.68.

Indoor situation investigations for an absorber tube with silver nanofluid along with a twisted tape insert were conducted by Waghole et al. [121]. Friction factor, thermal performance, and enhancement efficiency all were measured and reported. According to the research, the friction factor and Nusselt number of a smooth absorber tube rise by 1.0 to 1.75 times, and 1.25 to 2.10 times, respectively. In addition, the test revealed a 135% to 205% increase in enhancement efficiency.

Bellos et al. [122] used Al_2O_3-Water and Al_2O_3-Thermal oil nanofluids in a receiver tube to conduct numerical research. The receiver tube is of a converging–diverging type. According to the research, utilizing Al_2O_3-Thermal oil and Al_2O_3-Water fluid improves mean efficiency by 4.25% and 6.34%, respectively. Furthermore, the lowest pressure decrease was seen for water-based fluids with pressures ranging from 100 to 158 Pa. Furthermore, the scientists specifically state that the augmentation happened under high-temperature conditions.

In a PTSC receiver tube, Biswakarma et al. [123] looked at the effects of an Al2O3-Water nanofluid. The inside section of the receiver type has a helical groove. Six distinct nanofluid volume concentrations (3 to 8%) and three different critical heat flux values (600, 800, and 1000 W m^{-2}) were simulated together with two different Reynolds numbers (4000 and 6000). The heat transfer coefficient increases by 41.3% and the pressure decreases by 76.5% as the Reynolds number increases. Furthermore, the pressure drop increases by 14.5% in comparison with the base fluid when the volume concentration of nanoparticles is raised from 3 to 8%. Additionally, it was found that the greatest thermal improvement was 9% at an Al_2O_3 concentration of 8%. Smooth/plain absorber tubes have also been used in several investigations using nanofluids.

Extensive research has been carried out employing various nanofluids offered in PTSC's smooth/plain absorber tube. Moreover, several researchers are looking into the combined impact of nanofluid and insertion in absorber tubes. The use of nanofluid and performance study in modified absorber tubes having inserts and porous media are investigated. The use of nanofluids with inserts improves heat transmission significantly.

Using nanofluids in combination with turbulators (inserts and surface changes) results in a larger increase in thermal efficiency than using turbulators alone. Following is a list of advantages that may be determined after a comprehensive examination of nanofluid use as a heat transfer fluid in PTSC:

1. When compared to other metallic-based nanofluids, copper-based nanoparticles had the best thermal performance of all the nanoparticles studied. In a study conducted by Mahmoudi et al. [116], a receiver with a triangular cross section along with forwarding perforated ring steps was employed to achieve a thermal efficiency enhancement of 23.72%.
2. CNT nanoparticles provide the most thermal increase among non-metallic nanofluids. Kasaeian et al. [124] found that utilizing a 0.3% volume concentration of MWCNT in the absorber tube resulted in maximum thermal efficiency of 72.8%.
3. Nanofluid is often used in PTSC to increase heat transmission. Both the heat transfer coefficient and the Nusselt number have risen as a result of this increase.
4. Exergy efficiency is often increased when nanofluids are used. The combined usage of an annular porous structure and alumina put within the absorber tube resulted in a 15% increase in energy efficiency [125].

Conclusions

The purpose of the present article was to introduce and assess several heat transfer fluids that may be applied to PTC systems. By comparing many cutting-edge HTFs, this study aims to enhance the thermal performance of parabolic trough collector systems. Low pressure (1 atm), stability at high temperatures > 400 °C, low melting point, high thermal conductivity, high specific heat capacity or heat storage capacity, low dynamic viscosity, low corrosion rate, low toxicity, low cost, industrial availability, explosivity, and flammability are some of the thermophysical characteristics that influence the choice of HTF. Because thermal modifications to the physical system can only increase efficiency by 2% due to low thermal losses in the physical system, thermal properties like stability at high temperatures, thermal conductivity, melting point, and specific heat of HTF are a more promising option for increasing the thermal efficiency of PTC systems. An effective way to boost thermal efficiency is to employ HTF with remarkable thermophysical characteristics. Instead of employing water as the HTF, the system may use HTFs with larger latent heat capacities than water. The capacity of a nanofluid to conduct heat is diminished by agglomeration. As a result, both the Brownian motion of nanoparticles and the thermal performance of nanofluids are restricted. Hybrid nanofluids have greater thermal conductivity than monofluids. The geometry of nanoparticles affects their thermal conductivity (i.e., shape and size). In comparison with larger nanoparticles, a nanofluid with tiny-size nanoparticles has a higher concentration of nanoparticles overall. A base fluid with finer nanoparticles has more Brownian motion, which improves heat transfer. A nanofluid's viscosity rises with nanoparticle volume concentration and falls with temperature. During this viscosity reduction phase, the base fluid's nanoparticles become more quickly mobile, accelerating the rate of heat transfer and thermal conductivity. The key barriers to the commercialization of nanofluids are stability, production costs, the suitable selection of hybrid nanofluids, and pumping power. Nanofluids are likely to have a considerable impact on PTCs once these issues are recognized. One of the important elements influencing how a hybrid nanofluid manifests itself is stability; a nanofluid with low stability performs badly. The transition of nanofluid technology from small-scale testing to industrial production and commercialization may be sped up and systematized by solving all of the aforementioned issues. The highest thermal improvements are achieved with copper- and carbon-nanotube-based nanofluids. When nanoparticles are introduced to conventional fluids like water or oils, significant thermal increases occur. However, traditional fluids are a more reliable alternative owing to its user downsides, such as their high cost, instability problems, and collector rust.

1. CNT nanoparticles provide the most thermal increase among non-metallic nanofluids. Kasaeian et al. [91] found that utilizing a 0.3% volume concentration of MWCNT in the absorber tube resulted in maximum thermal efficiency of 72.8%.
2. Nanofluid is often used in PTSC to increase heat transmission. Both the heat transfer coefficient and the Nusselt number have risen as a result of this increase.
3. Exergy efficiency is often increased when nanofluids are used. The combined usage of an annular porous structure and alumina put within the absorber tube resulted in a 15% increase in energy efficiency [92].

The purpose of the present article was to introduce and assess several heat transfer fluids that may be applied to PTSC systems. By comparing many cutting-edge HTFs, this study aims to enhance the thermal performance of parabolic trough collector systems. Low pressure (1 atm), stability at high temperatures > 400 °C, low melting point, high thermal conductivity, high specific heat capacity or heat storage capacity, low dynamic viscosity, low corrosion rate, low toxicity, low cost, industrial availability, explosivity, and flammability are some of the thermophysical characteristics that influence the choice of HTF. Because thermal modifications to the physical system can only increase efficiency by 2% due to low thermal losses in the physical system, thermal properties like stability at high temperatures, thermal conductivity, melting point, and specific heat of HTF are a more promising option for increasing the thermal efficiency of PTC systems.

An effective way to boost thermal efficiency is to employ HTF with remarkable thermophysical characteristics. Instead of employing water as the HTF, the system may use HTFs with larger latent heat capacities than water. The capacity of a nanofluid to conduct heat is diminished by agglomeration. As a result, both the Brownian motion of nanoparticles and the thermal performance of nanofluids are restricted. Hybrid nanofluids have greater thermal conductivity than monofluids. The geometry of nanoparticles affects their thermal conductivity (i.e., shape and size). In comparison with larger nanoparticles, a nanofluid with tiny size nanoparticles has a higher concentration of nanoparticles overall. A base fluid with finer nanoparticles has more Brownian motion, which improves heat transfer. A nanofluid's viscosity rises with nanoparticle volume concentration and falls with temperature. During this viscosity reduction phase, the base fluid's nanoparticles become more quickly mobile, accelerating the rate of heat transfer and thermal conductivity. The key barriers to the commercialization of nanofluids are stability, production costs, the suitable selection of hybrid nanofluids, and pumping power. Nanofluids are likely to have a considerable impact on PTCs once these issues are recognized. One of the important elements influencing how a hybrid nanofluid manifests itself is stability; a nanofluid with low stability performs badly. The transition of nanofluid technology from small-scale testing to industrial production and commercialization may be sped up and systematized by solving all of the aforementioned issues. The highest thermal improvements are achieved with copper and carbon nanotube-based nanofluids. When nanoparticles are introduced to conventional fluids like water or oils, significant thermal increases occur. However, traditional fluids are a more reliable alternative owing to their user downsides, such as their high cost, instability problems, and collector rust.

Acknowledgements The corresponding author thankfully acknowledges the financial support from the All India Council of Technical Education Under the Research Promotion Scheme (RPS), the Government of India having research grant 8-46/FDC/RPS (POLICY-1)/2019-20 to carry out this project.

References

1. Cheng ZD, He YL, Xiao J, Tao YB, Xu RJ. Three-dimensional numerical study of heat transfer characteristics in the receiver tube of parabolic trough solar collector. Int Commun Heat Mass Transf. 2010;37:782–7. https://doi.org/10.1016/j.icheatmasstransfer.2010.05.002.
2. Qiu Y, Li M, He Y, Tao W. Thermal performance analysis of a parabolic trough solar collector using supercritical CO_2 as heat transfer fluid under non-uniform solar flux. Appl Therm Eng. 2016;115:1255–65. https://doi.org/10.1016/j.applthermaleng.2016.09.044.
3. Ray S, Tripathy AK, Sahoo SS, Bindra H. Performance analysis of receiver of parabolic trough solar collector: effect of selective coating, vacuum and semitransparent glass cover. Int J Energy Res. 2018;42:4235–49. https://doi.org/10.1002/er.4137.
4. Khanna S, Kedare SB, Singh S. Deflection and stresses in absorber tube of solar parabolic trough due to circumferential and axial flux variations on absorber tube supported at multiple points. Sol Energy. 2014;99:134–51. https://doi.org/10.1016/j.solener.2013.11.005.
5. Khanna S, Singh S, Kedare SB. Explicit expressions for temperature distribution and deflection in absorber tube of solar parabolic trough concentrator. Sol Energy. 2015;114:289–302. https://doi.org/10.1016/j.solener.2015.01.044.
6. Bhuyan U, Sahoo SS, Satapathy PK, Parida PK. Heat loss modelling and analysis of parabolic trough solar collector using computational approach. Aust J Mech Eng. 2019;17:24–37. https://doi.org/10.1080/14484846.2018.1507336.
7. Tripathy AK, Ray S, Sahoo SS, Chakrabarty S. Structural analysis of absorber tube used in parabolic trough solar collector and effect of materials on its bending: a computational study. Sol Energy. 2018;163:471–85. https://doi.org/10.1016/j.solener.2018.02.028.
8. Sahoo SS, Singh SS, Banerjee R. Thermal hydraulic simulation of absorber tubes in linear fresnel reflector solar thermal system using RELAP. Ren Energy. 2016;86:507–16. https://doi.org/10.1016/j.renene.2015.08.050.
9. Sahoo SS, Singh SS, Banerjee R. Steady sate hydrothermal analysis of absorber tubes used in Linear Fresnel Reflector solar thermal system. Sol Energy. 2013;87:84–95. https://doi.org/10.1016/j.solener.2012.10.002.
10. Sahoo SS, Varghese SM, Kumar CS, Viswanathan SP, Singh S, Banerjee R. Experimental investigation and computational validation of heat loss from the cavity receiver used in Linear Fresnel reflector solar thermal system. Renew Energy. 2013;55:18–23. https://doi.org/10.1016/j.renene.2012.11.036.
11. Sahoo SS, Singh S, Banerjee R. Analysis of heat loss from a trapezoidal cavity used for Linear Fresnel Reflector system. Sol Energy. 2012;86:1313–22. https://doi.org/10.1016/j.solener.2012.01.023.
12. Avargani VM, Norton B, Rahimi A. An open-aperture partially-evacuated receiver for more uniform reflected solar flux in circular-trough reflectors: comparative performance in air heating applications. Renew Energy. 2021;176:11–24. https://doi.org/10.1016/j.renene.2021.05.072.
13. Prakash M, Kedare SB, Nayak JK. Numerical study of natural convection loss from open cavities. Int J Therm Sci. 2012;51:23–30. https://doi.org/10.1016/j.ijthermalsci.2011.08.012.
14. Karimi R, Gheinani TT, Avargani VM. A detailed mathematical model for thermal performance analysis of a cylindrical cavity receiver in a solar parabolic dish collector system. Renew Energy. 2018;125:768–82. https://doi.org/10.1016/j.renene.2018.03.015.
15. Madadi V, Tavakoli T, Amir R. First and second thermodynamic law analyses applied to a solar dish collector. J Non-Equilib Thermodyn. 2014;39:183–97. https://doi.org/10.1515/jnet-2014-0023.
16. Avargani VM, Rahimi A, Tavakoli T. Exergetic optimization and optimum operation of a solar dish collector with a cylindrical receiver. J Energy Eng. 2016;142:04015049–51. https://doi.org/10.1061/(ASCE)EY.1943-7897.0000322.
17. Soltani S, Bonyadi M, Avargani VM. A novel optical-thermal modeling of a parabolic dish collector with a helically baffled cylindrical cavity receiver. Energy. 2019;168:88–98. https://doi.org/10.1016/j.energy.2018.11.097.

18. Karimi R, Gheinani TT, Avargani VM. Coupling of a parabolic solar dish collector to finned-tube heat exchangers for hot air production: an experimental and theoretical study. Sol Energy. 2019;187:199–211. https://doi.org/10.1016/j.solener.2019.05.050.
19. Avargani VM, Rahimi A, Divband M, Zamani MA. Optical analysis and heat transfer modeling of a helically baffled cavity receiver under solar flux non-uniformity and windy conditions. Therm Sci Eng Prog. 2020;20:100719. https://doi.org/10.1016/j.tsep.2020.100719.
20. Tagle-Salazar PD, Nigam KDP, Rivera-Solorio CI. Parabolic trough solar collectors: a general overview of technology, industrial applications, energy market, modeling, and standards. Green Process Synth. 2020;9:595–649. https://doi.org/10.1515/gps-2020-0059.
21. Coccia G, Di G, Sotte M. Design, manufacture, and test of a prototype for a parabolic trough collector for industrial process heat. Renew Energy. 2015;74:727–36. https://doi.org/10.1016/j.renene.2014.08.077.
22. Benoit H, Sprea L, Gauthier D, Flamant G. Review of heat transfer fluids in tube-receivers used in concentrating solar thermal systems: properties and heat transfer coefficients. Renew Sustain Energy Rev. 2016;55:298–315. https://doi.org/10.1016/j.rser.2015.10.059.
23. Aslfattahi N, Saidur R, Arifutzzaman A, Sadri R, Bimbo N, Sabri MFM, et al. Experimental investigation of energy storage properties and thermal conductivity of a novel organic phase change material/MXene as a new class of nanocomposites. J Energy Storage. 2020;27:101115. https://doi.org/10.1016/j.est.2019.101115.
24. Xiao P, Guo L, Zhang X. Investigations on heat transfer characteristic of molten salt flow in helical annular duct. Appl Therm Eng. 2015;88:22–32. https://doi.org/10.1016/j.applthermaleng.2014.09.021.
25. Shin D, Banerjee D. Enhanced thermal properties of SiO2 nanocomposite for solar thermal energy storage applications. Int J Heat Mass Transf. 2015;84:898–902. https://doi.org/10.1016/j.ijheatmasstransfer.2015.01.100.
26. Asadi A, Asadi M, Rezaniakolaei A, Rosendahl LA, Afrand M, Wongwises S. Heat transfer efficiency of Al2O3-MWCNT/thermal oil hybrid nanofluid as a cooling fluid in thermal and energy management applications: an experimental and theoretical investigation. Int J Heat Mass Transf. 2018;117:474–86. https://doi.org/10.1016/j.ijheatmasstransfer.2017.10.036.
27. Chieruzzi M, Miliozzi A, Crescenzi T, Torre L, Kenny JM. a new phase change material based on potassium nitrate with silica and alumina nanoparticles for thermal energy storage. Nanoscale Res Lett. 2015;10:273. https://doi.org/10.1186/s11671-015-0984-2.
28. Chieruzzi M, Cerritelli GF, Miliozzi A, Kenny JM. Effect of nanoparticles on heat capacity of nanofluids based on molten salts as PCM for thermal energy storage. Nanoscale Res Lett. 2013;8:1–9. https://doi.org/10.1186/1556-276X-8-448.
29. Chen YY, Zhao CY. Thermophysical properties of Ca (NO_3) 2-$NaNO_3$-KNO_3 mixtures for heat transfer and thermal storage. Sol Energy. 2017;146:172–9.
30. Sharma M, Jilte R. A review on passive methods for thermal performance enhancement in parabolic trough solar collectors. Int J Energy Res. 2021;45:4392–966. https://doi.org/10.1002/er.6212.
31. Avargani VM, Rahimi A, Divband M. Coupled optical and thermal analyses of a new type of solar water heaters using parabolic trough reflectors. Sustain Energy Technol Assess. 2020;40:100780. https://doi.org/10.1016/j.seta.2020.100780.
32. Avargani VM, Divband M. Performance evaluation of a solar water heating system with glass-covered parabolic trough concentrators, under different system tracking modes. J Therm Anal Calorim. 2022;147:4873–88. https://doi.org/10.1007/s10973-021-10845-9.
33. Sabiha MA, Saidur R, Mekhilef S, Mahian O. Progress and latest developments of evacuated tube solar collectors. Renew Sustain Energy Rev. 2015;51:1038–54. https://doi.org/10.1016/j.rser.2015.07.016.
34. Faizal M, Saidur R, Mekhilef S. Potential of size reduction of flat-plate solar collectors when applying Al_2O_3 nanofluid. Adv Mater Res. 2014;832:149–53. https://doi.org/10.4028/www.scientific.net/AMR.832.149.
35. Fernández-García A, Zarza E, Valenzuela L, Pérez M. Parabolic-trough solar collectors and their applications. Renew Sustain Energy Rev. 2010;14:1695–721. https://doi.org/10.1016/j.rser.2010.03.012.
36. Mahian O, Kianifar A, Kalogirou SA, Pop I, Wongwises S. A review of the applications of nanofluids in solar energy. Int J Heat Mass Transf. 2013;57:582–94. https://doi.org/10.1016/j.ijheatmasstransfer.2012.10.037.
37. Bellos E, Tzivanids C, Symeou C, Antonopoulos KA. Energetic, exergetic and financial evaluation of a solar driven absorption chiller – A dynamic approach. Energy Convers Manag. 2017;137:34–48. https://doi.org/10.1016/j.enconman.2017.01.041.
38. Silva R, Javier F, Pérez-garcía M. Process heat generation with parabolic trough collectors for a vegetables preservation industry in Southern Spain. Energy Procedia. 2014;48:1210–6. https://doi.org/10.1016/j.egypro.2014.02.137.
39. Giglio A, Lanzini A, Leone P, Rodríguez MM, Zarza E. Direct steam generation in parabolic-trough collectors: A review about the technology and a thermo-economic analysis of a hybrid system. Renew Sustain Energy Rev. 2017;74:453–73. https://doi.org/10.1016/j.rser.2017.01.176.
40. Selvakumar P, Somasundaram P, Thangavel P. Performance study on evacuated tube solar collector using therminol D-12 as heat transfer fluid coupled with parabolic trough. Energy Convers Manag. 2014;85:505–10. https://doi.org/10.1016/j.enconman.2014.05.069.
41. Raade JW, Padowitz D. Development of molten salt heat transfer fluid with low melting point and high thermal stability. ASME J Sol Energy Eng. 2011;133:031013. https://doi.org/10.1115/1.4004243.
42. Zhang HL, Baeyens J, Degrève J, Cacères G. Concentrated solar power plants: review and design methodology. Renew Sustain Energy Rev. 2013;22:466–81. https://doi.org/10.1016/j.rser.2013.01.032.
43. Wang Y, Liu Q, Lei J, Jin H. A three-dimensional simulation of a parabolic trough solar collector system using molten salt as heat transfer fluid. Appl Therm Eng. 2014;70:462–76. https://doi.org/10.1016/j.applthermaleng.2014.05.051.
44. Bauer T, Pfleger N, Laing D, Eck M, Kaesche S. 20 high-temperature molten salts for solar power application. Molten Salts Chem. 2013;2013:415–38. https://doi.org/10.1016/B978-0-12-398538-5.00020-2.
45. Coscia K, Elliott T, Mohapatra S, Oztekin A, Neti S. Binary and ternary nitrate solar heat transfer fluids. ASME J Sol Energy Eng. 2013;135:021011. https://doi.org/10.1115/1.4023026.
46. Chen M, Shen Y, Zhu S, Li P. Digital phase diagram and thermophysical properties of KNO_3-$NaNO_3$-$Ca(NO_3)_2$ ternary system for solar energy storage. Vacuum. 2017;145:225–33. https://doi.org/10.1016/j.vacuum.2017.09.003.
47. Fernández AG, Ushak S, Galleguillos H, Pérez FJ. Development of new molten salts with $LiNO_3$ and $Ca(NO_3)_2$ for energy storage in CSP plants. Appl Energy. 2014;119:131–40. https://doi.org/10.1016/j.apenergy.2013.12.061.

48. Vignarooban K, Xu X, Arvay A, Hsu K, Kannan AM. Heat transfer fluids for concentrating solar power systems - a review. Appl Energy. 2015;146:383–96. https://doi.org/10.1016/j.apenergy.2015.01.125.
49. Zhao CY, Wu ZG. Thermal property characterization of a low melting-temperature ternary nitrate salt mixture for thermal energy storage systems. Sol Energy Mater Sol Cells. 2011;95:3341–6. https://doi.org/10.1016/j.solmat.2011.07.029.
50. Chieruzzi M, Miliozzi A, Crescenzi T, Torre L, Kenny JM. A new phase change material based on potassium nitrate with silica and alumina nanoparticles for thermal energy storage. Nanoscale Res Lett. 2015. https://doi.org/10.1186/s11671-015-0984-2.
51. Chen YY, Zhao CY. Thermophysical properties of $Ca(NO_3)2$-$NaNO_3$-KNO_3 mixtures for heat transfer and thermal storage. Sol Energy. 2017;146:172–9. https://doi.org/10.1016/j.solener.2017.02.033.
52. Yarmand H, Gharehkhani S, Shirazi SFS, Goodarzi M, Amiri A, Sarsam WS, et al. Study of synthesis, stability and thermo-physical properties of graphene nanoplatelet/platinum hybrid nanofluid. Int Commun Heat Mass Transf. 2016;77:15–21. https://doi.org/10.1016/j.icheatmasstransfer.2016.07.010.
53. Wei B, Zou C, Li X. Experimental investigation on stability and thermal conductivity of diathermic oil based TiO_2 nanofluids. Int J Heat Mass Transf. 2017;104:537–43. https://doi.org/10.1016/j.ijheatmasstransfer.2016.08.078.
54. Ilyas SU, Pendyala R, Narahari M. Stability and thermal analysis of MWCNT-thermal oil-based nanofluids. Colloids Surf A Physicochem Eng Asp. 2017;527:11–22. https://doi.org/10.1016/j.colsurfa.2017.05.004.
55. Wang T, Mantha D, Reddy RG. Novel low melting point quaternary eutectic system for solar thermal energy storage. Appl Energy. 2013;102:1422–9. https://doi.org/10.1016/j.apenergy.2012.09.001.
56. Bradshaw RW, Brosseau DA. Low-melting point inorganic nitrate salt heat transfer fluid. United States Pat US 7,588,694 B1 2009. pp. 1–9.
57. Peng Q, Yang X, Ding J, Wei X, Yang J. Design of new molten salt thermal energy storage material for solar thermal power plant. Appl Energy. 2013;112:682–9. https://doi.org/10.1016/j.apenergy.2012.10.048.
58. Good P, Zanganeh G, Ambrosetti G, Barbato MC, Pedretti A, Steinfeld A. Towards a commercial parabolic trough CSP system using air as heat transfer fluid. Energy Procedia. 2014;49:381–5. https://doi.org/10.1016/j.egypro.2014.03.041.
59. Bellos E, Tzivanidis C, Antonopoulos KA, Daniil I. The use of gas working fluids in parabolic trough collectors – an energetic and exergetic analysis. Appl Therm Eng. 2016;109:1–14. https://doi.org/10.1016/j.applthermaleng.2016.08.043.
60. Al-Sulaiman FA, Zubair MI, Atif M, Gandhidasan P, Al-Dini SA, Antar MA. Humidification dehumidification desalination system using parabolic trough solar air collector. Appl Therm Eng. 2015;75:809–16. https://doi.org/10.1016/j.applthermaleng.2014.10.072.
61. Biencinto M, González L, Valenzuela L, Zarza E. A new concept of solar thermal power plants with large-aperture parabolic-trough collectors and CO_2 as working fluid. Energy Convers Manag. 2019;199:112030. https://doi.org/10.1016/j.enconman.2019.112030.
62. Islam MK, Hasanuzzaman M, Rahim NA. RSC Modelling and analysis of the effect of different parameters on a parabolic-trough concentrating solar system. RSC Adv. 2015. https://doi.org/10.1039/C4RA12919A.
63. Vutukuru R, Pegallapati AS, Maddali R. Suitability of various heat transfer fluids for high temperature solar thermal systems. Appl Therm Eng. 2019;159:113973. https://doi.org/10.1016/j.applthermaleng.2019.113973.
64. Pacio J, Singer C, Wetzel T, Uhlig R. Thermodynamic evaluation of liquid metals as heat transfer fluids in concentrated solar power plants. Appl Therm Eng. 2013;60:295–302. https://doi.org/10.1016/j.applthermaleng.2013.07.010.
65. Sarafraz MM, Arjomandi M. Demonstration of plausible application of gallium nano-suspension in microchannel solar thermal receiver: experimental assessment of thermo- hydraulic performance of microchannel. Int Commun Heat Mass Transf. 2018;94:39–46. https://doi.org/10.1016/j.icheatmasstransfer.2018.03.013.
66. Paul TC, Morshed AKMM, Fox EB, Khan JA. Thermal performance of Al_2O_3 nanoparticle enhanced ionic liquids (NEILs) for concentrated solar power (CSP) applications. Int J Heat Mass Transf. 2015;85:585–94. https://doi.org/10.1016/j.ijheatmasstransfer.2015.01.071.
67. Sanada Y, Akiba I, Hashida S, Sakurai K, et al. Composition dependence of the micellar architecture made from poly(ethylene glycol)-block-poly(partially benzyl-esterified aspartic acid). J Phys Chem B. 2012;116:8241–50. https://doi.org/10.1021/jp300936d.
68. Moens L, Blake DM. Advanced heat transfer and thermal storage fluids. Conference paper NREL/CP-510-37083 2005.
69. Wittmar A, Ruiz-Abad D, Ulbricht M. Dispersions of silica nanoparticles in ionic liquids investigated with advanced rheology. J Nanoparticle Res. 2012;14:1–10. https://doi.org/10.1007/s11051-011-0651-1.
70. Wang B, Wang X, Lou W, Hao J. Ionic liquid-based stable nanofluids containing gold nanoparticles. J Colloid Interface Sci. 2011;362:5–14. https://doi.org/10.1016/j.jcis.2011.06.023.
71. Perissi I, Bardi U, Caporali S, Fossati A, Lavacchi A. Ionic liquids as diathermic fluids for solar trough collectors' technology: a corrosion study. Sol Energy Mater Sol Cells. 2008;92:510–7. https://doi.org/10.1016/j.solmat.2007.11.007.
72. Liu J, Ye Z, Zhang L, Fang X, Zhang Z. Solar energy materials & solar cells A combined numerical and experimental study on graphene/ionic liquid nano fluid based direct absorption solar collector. Sol Energy Mater Sol Cells. 2015;136:177–86. https://doi.org/10.1016/j.solmat.2015.01.013.
73. Hoffmann JF, Vaitilingom G, Henry JF, Chirtoc M, Olives R, Goetz V, Py X. Temperature dependence of thermophysical and rheological properties of seven vegetable oils in view of their use as heat transfer fluids in concentrated solar plants. Sol Energy Mater Sol Cells. 2018;178:129–38. https://doi.org/10.1016/j.solmat.2017.12.037.
74. Aberoumand S, Jafarimoghaddam A. Tungsten (III) oxide (WO3) – Silver/transformer oil hybrid nanofluid: preparation, stability, thermal conductivity and dielectric strength. Alex Eng J. 2018;57:169–74. https://doi.org/10.1016/j.aej.2016.11.003.
75. Hemmat Esfe M, Abbasian Arani AA, Rezaie M, Yan WM, Karimipour A. Experimental determination of thermal conductivity and dynamic viscosity of Ag–MgO/water hybrid nanofluid. Int Commun Heat Mass Transf. 2015;66:189–95. https://doi.org/10.1016/j.icheatmasstransfer.2015.06.003.
76. Yang L, Ji W, Mao M, Huang JN. An updated review on the properties, fabrication and application of hybrid-nanofluids along with their environmental effects. J Clean Prod. 2020;257:120408. https://doi.org/10.1016/j.jclepro.2020.120408.
77. Suresh S, Venkitaraj KP, Selvakumar P, Chandrasekar M. Synthesis of Al2O3-Cu/water hybrid nanofluids using two step method and its thermo physical properties. Colloids Surf A Physicochem Eng Asp. 2011;388:41–8. https://doi.org/10.1016/j.colsurfa.2011.08.005.
78. Chen LF, Cheng M, Yang DJ, Yang L. Enhanced thermal conductivity of nanofluid by synergistic effect of multi-walled carbon nanotubes and Fe2O3 nanoparticles. Appl Mech Mater.

2014;548–549:118–23. https://doi.org/10.4028/www.scientific.net/AMM.548-549.118.
79. Timofeeva EV, Gavrilov AN, McCloskey JM, Tolmachev YV, Sprunt S, Lopatina LM, et al. Thermal conductivity and particle agglomeration in alumina nanofluids: Experiment and theory. Phys Rev E Stat Nonlinear Soft Matter Phys. 2007;76:28–39. https://doi.org/10.1103/PhysRevE.76.061203.
80. Le Ba T, Mahian O, Wongwises S, Szilágyi IM. Review on the recent progress in the preparation and stability of graphene-based nanofluids. J Therm Anal Calorim. 2020;142:1145–72. https://doi.org/10.1007/s10973-020-09365-9.
81. Suresh S, Venkitaraj KP, Selvakumar P, Chandrasekar M. Effect of Al_2O_3-Cu/water hybrid nanofluid in heat transfer. Exp Therm Fluid Sci. 2012;38:54–60. https://doi.org/10.1016/j.expthermflusci.2011.11.007.
82. Sanchez C, Julián B, Belleville P, Popall M. Applications of hybrid organic-inorganic nanocomposites. J Mater Chem. 2005;15:3559–92. https://doi.org/10.1039/b509097k.
83. Bhosale GH, Borse SL. Pool boiling CHF enhancement with Al_2O_3-Cuo/H_2O hybrid Nan fluid. Int J Eng Res Technol. 2013;2:946–50.
84. Dhinesh Kumar D, Valan AA. A comprehensive review of preparation, characterization, properties and stability of hybrid nanofluids. Renew Sustain Energy Rev. 2018;81:1669–89. https://doi.org/10.1016/j.rser.2017.05.257.
85. Cakmak NK, Said Z, Sundar LS, Ali ZM, Tiwari AK. Preparation, characterization, stability, and thermal conductivity of rGO-Fe_3O_4-TiO_2 hybrid nanofluid: an experimental study. Powder Technol. 2020;372:235–45. https://doi.org/10.1016/j.powtec.2020.06.012.
86. Qiu L, Zhu N, Feng Y, Michaelides EE, Żyła G, Jing D, et al. A review of recent advances in thermophysical properties at the nanoscale: from solid state to colloids. Phys Rep. 2020;843:1–81. https://doi.org/10.1016/j.physrep.2019.12.001.
87. Paul G, Pal T, Manna I. Thermo-physical property measurement of nano-gold dispersed water based nanofluids prepared by chemical precipitation technique. J Colloid Interface Sci. 2010;349:434–7. https://doi.org/10.1016/j.jcis.2010.05.086.
88. Gupta M, Singh V, Kumar S, Kumar S, Dilbaghi N, Said Z. Up to date review on the synthesis and thermophysical properties of hybrid nanofluids. J Clean Prod. 2018;190:169–92. https://doi.org/10.1016/j.jclepro.2018.04.146.
89. Montes MJ. Thermofluidynamic model and comparative analysis of parabolic trough collectors using oil. Water Steam Molten Salt. 2014;132:1–7. https://doi.org/10.1115/1.4001399.
90. Fritsch A, Frantz C, Uhlig R. Techno-economic analysis of solar thermal power plants using liquid sodium as heat transfer fluid. Sol Energy. 2019;177:155–62. https://doi.org/10.1016/j.solener.2018.10.005.
91. Mahian O, Kolsi L, Amani M, Estellé P, Ahmadi G, Kleinstreuer C, et al. Recent advances in modeling and simulation of nanofluid flows-Part I: fundamentals and theory. Phys Rep. 2019;790:1–48. https://doi.org/10.1016/j.physrep.2018.11.004.
92. Corcione M. Empirical correlating equations for predicting the effective thermal conductivity and dynamic viscosity of nanofluids. Energy Convers Manag. 2011;52:789–93. https://doi.org/10.1016/j.enconman.2010.06.072.
93. Prasher R, Song D, Wang J, Phelan P. Measurements of nanofluid viscosity and its implications for thermal applications. Appl Phys Lett. 2006;89:67–70. https://doi.org/10.1063/1.2356113.
94. De Noni A, Garcia DE, Hotza D. A modified model for the viscosity of ceramic suspensions. Ceram Int. 2002;28:731–5. https://doi.org/10.1016/S0272-8842(02)00035-4.
95. Novotny V, Meincke PPM, Watson JHP. Effect of size and surface on the specific heat of small lead particles. Phys Rev Lett. 1972;28:901–3. https://doi.org/10.1103/PhysRevLett.28.901.
96. Angayarkanni SA, Philip J. Review on thermal properties of nanofluids: recent developments. Adv Colloid Interface Sci. 2015;225:146–76. https://doi.org/10.1016/j.cis.2015.08.014.
97. Riazi H, Murphy T, Webber GB, Atkin R, Tehrani SSM, Taylor RA. Specific heat control of nanofluids: a critical review. Int J Therm Sci. 2016;107:25–38. https://doi.org/10.1016/j.ijthermalsci.2016.03.024.
98. Abbasi M, Heyhat MM, Rajabpour A. Study of the effects of particle shape and base fluid type on density of nanofluids using ternary mixture formula: a molecular dynamics simulation. J Mol Liq. 2020;305:112831. https://doi.org/10.1016/j.molliq.2020.112831.
99. Chavan D, Pise A. Experimental investigation of effective viscosity and density of nanofluids. Mater Today Proc. 2019;16:504–15. https://doi.org/10.1016/j.matpr.2019.05.122.
100. Sundar LS, Sharma KV, Singh MK, Sousa ACM. Hybrid nanofluids preparation, thermal properties, heat transfer and friction factor – a review. Renew Sustain Energy Rev. 2017;68:185–98. https://doi.org/10.1016/j.rser.2016.09.108.
101. Bakthavatchalam B, Habib K, Saidur R, Saha BB, Irshad K. Comprehensive study on nanofluid and ionanofluid for heat transfer enhancement: a review on current and future perspective. J Mol Liq. 2020;305:112787. https://doi.org/10.1016/j.molliq.2020.112787.
102. Zhu T, Strycker A, Raible CJ, Vineyard K. Foams for mobility control and improved sweep efficiency in gas flooding 1998. pp. 277–86. https://doi.org/10.2118/39680-ms
103. Farajzadeh R, Andrianov A, Zitha PLJ. Investigation of immiscible and miscible foam for enhancing oil recovery. Ind Eng Chem Res. 2010;49:1910–9. https://doi.org/10.1021/ie901109d.
104. Babar H, Ali HM. Towards hybrid nanofluids: Preparation, thermophysical properties, applications, and challenges. J Mol Liq. 2019;281:598–633. https://doi.org/10.1016/j.molliq.2019.02.102.
105. Saidur R, Leong KY, Mohammed HA. A review on applications and challenges of nanofluids. Renew Sustain Energy Rev. 2011;15:1646–68. https://doi.org/10.1016/j.rser.2010.11.035.
106. Alirezaie A, Hajmohammad MH, Hassani Ahangar MR, Hemmat EM. Price-performance evaluation of thermal conductivity enhancement of nanofluids with different particle sizes. Appl Therm Eng. 2018;128:373–80. https://doi.org/10.1016/j.applthermaleng.2017.08.143.
107. Olia H, Torabi M, Bahiraei M, Ahmadi MH, Goodarzi M, Safaei MR. Application of nanofluids in thermal performance enhancement of parabolic trough solar collector: state-of-the-art. Appl Sci. 2019. https://doi.org/10.3390/app9030463.
108. Mwesigye A, Huan Z, Meyer JP. Thermodynamic optimisation of the performance of a parabolic trough receiver using synthetic oil-Al2O3 nanofluid. Appl Energy. 2015;156:398–412. https://doi.org/10.1016/j.apenergy.2015.07.035.
109. Shah TR, Ali HM. Applications of hybrid nanofluids in solar energy, practical limitations and challenges: a critical review. Sol Energy. 2019;183:173–203. https://doi.org/10.1016/j.solener.2019.03.012.
110. Sundar LS, Singh MK, Sousa ACM. Enhanced heat transfer and friction factor of MWCNT-Fe_3O_4/water hybrid nanofluids. Int Commun Heat Mass Transf. 2014;52:73–83. https://doi.org/10.1016/j.icheatmasstransfer.2014.01.012.
111. Biswas N, Manna NK, Datta P, Mahapatra PS. Analysis of heat transfer and pumping power for bottom-heated porous cavity saturated with Cu-water nanofluid, vol. 326. Amsterdam: Elsevier; 2018. https://doi.org/10.1016/j.powtec.2017.12.030.
112. Rahmanian S, Hamzavi A. Effects of pump power on performance analysis of photovoltaic thermal system using CNT nanofluid. Sol Energy. 2020;201:787–97. https://doi.org/10.1016/j.solener.2020.03.061.

113. Chamsa-ard W, Brundavanam S, Fung CC, Fawcett D, Poinern G. Nanofluid types, their synthesis, properties and incorporation in direct solar thermal collectors: a review. Nanomaterials. 2017. https://doi.org/10.3390/nano7060131.
114. Bellos E, Tzivanidis C. A review of concentrating solar thermal collectors with and without nanofluids. J Therm Anal Calorim. 2019;135:763–86. https://doi.org/10.1007/s10973-018-7183-1.
115. Krishna Y, Faizal M, Saidur R, Ng KC, Aslfattahi N. State-of-the-art heat transfer fluids for parabolic trough collector. Int J Heat Mass Transf. 2020. https://doi.org/10.1016/j.ijheatmasstransfer.2020.119541.
116. Mahmoudi A, Fazli M, Morad MR, Gholamalizadeh E. Thermo-hydraulic performance enhancement of nanofluid-based linear solar receiver tubes with forward perforated ring steps and triangular cross section; a numerical investigation. Appl Therm Eng. 2020;169:114909. https://doi.org/10.1016/j.applthermaleng.2020.114909.
117. Rostami S, Rostami S, Shahsavar A, Shahsavar A, Kefayati G, Goldanlou AS, et al. Energy and exergy analysis of using turbulator in a parabolic trough solar collector filled with mesoporous silica modified with copper nanoparticles hybrid nanofluid. Energies. 2020. https://doi.org/10.3390/en13112946.
118. Bilal FR, Arunachala UC, Sandeep HM. Experimental validation of energy parameters in parabolic trough collector with plain absorber and analysis of heat transfer enhancement techniques. J Phys Conf Ser. 2018. https://doi.org/10.1088/1742-6596/953/1/012030.
119. Hatami M, Geng J, Jing D. Enhanced efficiency in concentrated parabolic solar collector (CPSC) with a porous absorber tube filled with metal nanoparticle suspension. Green Energy Environ. 2018;3:129–37. https://doi.org/10.1016/j.gee.2017.12.002.
120. Amina B, Miloud A, Samir L, Abdelylah B, Solano JP. Heat transfer enhancement in a parabolic trough solar receiver using longitudinal fins and nanofluids. J Therm Sci. 2016;25:410–7. https://doi.org/10.1007/s11630-016-0878-3.
121. Waghole DR, Warkhedkar RM, Kulkarni VS, Shrivastva RK. Experimental investigations on heat transfer and friction factor of silver nanofliud in absorber/receiver of parabolic trough collector with twisted tape inserts. Energy Procedia. 2014;45:558–67. https://doi.org/10.1016/j.egypro.2014.01.060.
122. Bellos E, Tzivanidis C, Antonopoulos KA, Gkinis G. Thermal enhancement of solar parabolic trough collectors by using nanofluids and converging-diverging absorber tube. Renew Energy. 2016;94:213–22. https://doi.org/10.1016/j.renene.2016.03.062.
123. Biswakarma S, Roy S, Das B, Kumar DB. Performance analysis of internally helically v-grooved absorber tubes using nanofluid. Therm Sci Eng Prog. 2020;18:100538. https://doi.org/10.1016/j.tsep.2020.100538.
124. Kasaeian A, Daneshazarian R, Rezaei R, Pourfayaz F, Kasaeian G. Experimental investigation on the thermal behavior of nanofluid direct absorption in a trough collector. J Clean Prod. 2017;158:276–84. https://doi.org/10.1016/j.jclepro.2017.04.131.
125. Bozorg MV, Hossein Doranehgard M, Hong K, Xiong Q. CFD study of heat transfer and fluid flow in a parabolic trough solar receiver with internal annular porous structure and synthetic oil–Al2O3 nanofluid. Renew Energy. 2020;145:2598–614. https://doi.org/10.1016/j.renene.2019.08.042.